AAiT

Addis Ababa Institute of Technology
አዲስ አበባ ቴክኖሎጂ ኢንስቲትዩት
Addis Ababa University
አዲስ አበባ ዩኒቨርሲቲ

SCHOOL OF MECHANICAL AND INDUSTRIAL ENGINEERING

MASTERS OF RAILWAY ENGINEERING

Stability of trains under aerodynamic excitation for Addis Ababa Light railway transit (A.A.L.R.T)

A Thesis Submitted To the Graduate School of Addis Ababa University in Partial Fulfilment of the Requirement for the Degree of Masters of Science

In Mechanical Engineering

By: - Abel Demissie

Advisor: -Mr. Habtamu Tkubet

May,2015

ADDIS ABABA UNIVERSITY

Addis Ababa Institute of Technology

School of Mechanical and Industrial Engineering

(Stream: Mechanical Railway Engineering)

Master's Program Final Thesis Acceptance Approval Form

Thesis Topic: Stability of trains under aerodynamic excitation for Addis Ababa Light Railway Transit (A.A.L.R.T)

By: Abel Demissie

Approved By Board Of Examiners:

Mr. Habtamu Tkubet	_____	_____
Advisor	Signature	Date
Mr. Tolossa Deberie	_____	_____
Internal Examiner	Signature	Date
Dr. Daniel Tilahun	_____	_____
External Examiner	Signature	Date
Dr. Birhanu Beshah	_____	_____
Railway Head Center	Signature	Date

Declaration

I, the undersigned, declare that this thesis report entitled-"**Stability of trains under aerodynamic excitation for A.A.L.R.T"** is the result of my own research carried out under the supervision of Mr. Habtamu Tkubet. It has not been presented as a thesis in any other university and all source of material used for this thesis are fully acknowledged.

Abel Demissie _____ Date _____

This is to certify that the above declaration made by the candidate is correct to the best of my knowledge.

Habtamu Tkubet _____ Date _____

[Advisor]

Acknowledgement

First and foremost I thank almighty God, and then I would like to extend my gratitude to my advisor Mr. Habtamu Tkubet and the school of Mechanical Engineering. I would also like to thank ERC for this graduate opportunity and for providing crucial data, without it this project would not have been possible. I would also like to thank my family and colleagues for their support and insightful comments regarding this paper.

Abstract

Railway train aerodynamic problems are closely associated with the flows occurring around train. This work is based on numerical model using Computational Fluid Dynamics (CFD) approach to obtain the impact of air flow around a train operating in selected scenarios. These scenarios are train passing each other and train passing through the tunnel. The model of generic passenger train was developed using CatiaV5 and generated the wind tunnel and applied the boundary conditions in ANSYS workbench 13.0. The simulation work of the test vehicle and grid system is constructed by ANSYS-13.0. FLUENT which is the CFD solver and employed in the present work. In this study, numerical iterations are completed, then after aerodynamic data and detailed complicated flow structure are visualized

The paper aimed at investigating the aerodynamic impact on a lightweight railway vehicle used in A.A.LRT. The performed simulation allows measuring the aerodynamic forces on the vehicles. Numerical prediction of incompressible flow has been performed in AALRT train moving at a speed of 22.2m/s (80k/hr). Fluent, the CFD code which incorporates K-ε turbulence model and segregated implicit solver was used for the computation.

The aerodynamic analysis was performed to study the flow behavior of the air over the train body. The analysis includes the study of contours of pressure and velocity. The peak pressure difference along the train is 1615KPa which is exhibited for trains passing each other. The two scenarios conducted for a train exiting and entering the tunnel shows that the pressure deviation is very low with a magnitude of 1411Kpa and 1355Kp respectively

Table of Contents

List of Figures

List of tables

Nomenclature

A.A.L.R.T Addis Ababa Light Railway Transit

E.R.C Ethiopian Railway Corporation

CFD computational fluid dynamics

RANS Reynolds Aggregated numerical simulation

a speed of sound or constant

A Cross-sectional area of tunnel

A_0 cross-sectional area of train

c speed of sound or constant

Cd aerodynamic drag coefficient

C_{ds} aerodynamic drag coefficient of short model train

C_{dl} aerodynamic drag coefficient of long model train

C_{dp} pressure drag coefficient

D Total drag

D_M mechanical drag

D_A aerodynamic drag

E Energy

f Frictional force on train

F frictional force on tunnel wall

H Height of train

c train length

m' mass flow per unit time per unit volume

M_t train Mach number

M mass flow per unit time

P static pressure

D_{p0} pressure difference

r radial distance

Re Reynolds number

S Struve function

t time

u flow velocity

u_0 flow velocity between train and tunnel wall

U speed of train

V speed of train

W_p payload

W weight of train

x axial distance of tunnel

Greek letters

α Angle of attack

γ Ratio of specific heat

ρ Density

λ Friction wall factor

λ' Friction factor of the train

$\lambda_m{}'$ Friction factor of train model

φ Energy dissipation

ϕ Velocity potential

υ Kinetic viscosity

Chapter 1

1. Introduction

Trains have been a part of modern transportation system for more than a century. The railway train running along a track is one of the most complicated dynamical systems in engineering. Many bodies comprise the system and so it has many degrees of freedom. The bodies that make up the vehicle can be connected in various ways and a moving interface connects the vehicle with the track. [1]

1.1. History of railway and the development of A.A.L.R.T in Ethiopia

Railway was introduced to Ethiopia in the early 19th century with the idea of constructing a railway link between Addis Ababa with the coast of Djibouti. The first train service began on July 22, 1901, and operated between Djibouti and Douanle, the first station on the Ethiopian side of the frontier at 106 kilometer, a journey of 5 1/2 hours with four halts for water. A year and a half later the service was extended as far as Dire Dawa, 14 hours from the coast at kilometer 311. The first train reached that town, which was long destined to be the terminus of the line, on December 24, 1902 having passed 13 stations in the route. [2]

However, its development has been stagnant. Until recently, Ethiopia has one semi functioning railway route that connects Addis Ababa to Djibouti through Dire-Dawa. Nowadays, Ethiopia is undertaking a massive railway project in National Railway Network [N.R.T] and Light railway transit for the city of Addis Ababa [AALRT]. The newly designed and implemented A.A.L.R.T is Metropolitan electric railway with a total length of 34.25 km (North South line 16.9 km and East-West line 17.35 km). These two lines (North-South and East West lines) use common track of about 2.7 km. It's designed with Track Gauge of 1435mm and Maximum Service Speed: 80 km/h. [3]

1.2. Aerodynamics and Railway Industries

The aerodynamics of railway vehicles covers a wide range topics reaching from the aerodynamic loads acting on structure and components of the train, the flow characteristics around the train influencing the efficiency of mechanical components and the aerodynamic influence of the train and its infrastructure. All these effects need to be investigated to ensure an efficient layout of the train in manufacturing, maintenance and operation. The specific description of the aerodynamic loads on a railway vehicle is one of the most relevant tasks for the construction and operation of modern trains. [4]

The vehicle aerodynamics have become crucial since have realized its importance. The tools used have been set to their optimum size, angle and shape to achieve the best. Next to reduction in the drag coefficient, lift coefficient has also been investigated and enhanced for better performance. The physical appearance of the vehicle has been given keen significance while designing the external devices. [5]

The shape of vehicles changed in a revolutionary manner over the past few years as aerodynamics concept started to be adopted for road vehicles and trains. Exterior design (the term "styling" that was formerly used is now avoided) and started to be recognized as extremely important. [6] While design gives technical requirements a form that is in accord with both technical requirement and aesthetical value and consequently vehicle aerodynamics is getting better and better. Improved performance and efficient operation is the major concern of railway industries.

Traditionally less emphasis was given to aerodynamic impact, as the benefits of aerodynamics were simply negligible. Nowadays the railway industry is very keen to address the negative influence of aerodynamics. The need for increased performance standards, there is growing emphases on effective designs that reduce drag force impact as well develop a guideline for safe operation that would help to minimize the negative effect of aerodynamic forces. With a desire to have faster and efficient trains, their design and manufacturing of rail vehicle has to address the effect aerodynamics impacts such as drag, cross (side) wind. It’s also advised to make Train be lighter in order to reduce energy requirement. Although trains in past were probably

unnecessarily heavy, cutting in weight must be done with largest possible care in order to retain train's stability. [7]

The train has to be resistant to undesirable positional change. Even in the presence of forces that would interfere with the motion of the train, the train has to maintain equilibrium. The unsteadiness and the different forces and moments that start acting on the train have a big impact on the stability of the train and safety and comfort of the passengers. [8] They can disturb the normal operation, cause damages in the infrastructures or even accidents like derailment or overturning.

Depending on the specific purpose of each type of rail vehicle, the impact of aerodynamics differs widely. While low drag is desirable, it is not only one of the aerodynamic forces acting on rail vehicles and other aerodynamic properties such as static and dynamic pressure, aero acoustics noise and upraise of ballast due to flow have significant impact on train dynamics. Many attempts have been made since the early years in the automotive and railway industries to reduce aerodynamic drag in order to improve performance and stability. [9]

This research will attempt to simulate aerodynamic impacts on trains at the newly built A.A.L.R.T. In order to perform this task, different scenarios were selected in accordance with susceptibility for high aerodynamic impacts to assess the overall impact of aerodynamic forces on train stability and propose methods that can improve up on any bad impacts that are created as a result. The two prominent scenarios chosen for this study are when two trains pass each other in an open field and when a train passes through a tunnel. A scenario with a tunnel is selected due to concentrated airflow around tunnel entrance and exiting which in turn lead to higher aerodynamic load. The scenario where two trains are passing each other also exhibit higher aerodynamic load as the direction air flow is affected by the existence of two train bodies at a particular insistence when the two trains meet.

1.3. Objective of the study

1.3.1. General objective

To assess the overall impact of aerodynamic forces on train stability and propose methods that can improve up on any bad impacts that are created as a result

1.3.2. Specific objective

- ✓ To determine the aerodynamic forces and moments affecting the train and their effects on discomfort and instability.
- ✓ Determine the static and dynamic pressure distribution on the train body.
- ✓ Aerodynamic evaluation of air flow over an object can be performed using CFD approach.
- ✓ Measure the undesired drag force in the given scenarios

1.4. Significance of the study

The primary merit of the study goes to ERC future research center. It can be extrapolated for operational purpose serving as an input for designing guidelines. The railway system is new to our country and studies are bound to be conducted on the rail system and this paper can give a certain starting point for more advanced researches. The insights obtained from this research in the field rail vehicle aerodynamics would serve as input when designing and manufacturing of rail vehicles is extensively exercised in the country.

1.5. Scope of the study

This research studies aerodynamic interaction of trains and their effect on train operation fully focused on the Addis Ababa Light Rail transit (A.A.L.R.T). CFD model and simulation of the aerodynamic interaction would show the overall aerodynamic interaction. The study only focus on 3d modeling and simulation as experimentation is not viable

1.6. Limitation of the study

This study would be conducted in the new A.A.L.R.T system. While this addresses the relevance of the study to the existing need, the fact the railway operation is yet to be operational have a significant limitation in terms of selecting the desirable scenarios of which severe aerodynamic impacts are observed. This paper only focuses on simulation as conducting experiments unfeasible due to time and other constraints.

1.7. Methodology of the Research

1.7.1. Data collection

For this study, Primary as well as secondary data will be required. However, due to the fact that A.A.L.R.T is yet to be operational, getting primary data can be difficult. The principal primary data for this study would be an observation made on the selected routes and real life conditions of the infrastructure. Apart from this observation, the study will heavily rely on second data. These include:

- ✓ Published articles on the subject matter, related thesis paper, websites and journals
- ✓ Data from ERC(proposed design of the vehicles to approximate the overall vehicle behavior)
- ✓ Researches that are performed on this topic.

1.7.2. Data analysis

The research is focused on the actual conditions, both geographical and operational; In order to perform this task, different scenarios will be selected.

i. A scenario where two trains passes each other.

ii. A scenario when a train goes in to the tunnel, when a train passes through a tunnel, pressure waves are propagated in the tunnel. If the train is not absolutely pressure-tight, these pressure changes are partly transmitted inside the train and may be uncomfortable for the passengers.

One of the most important requirements before carrying out a CFD computation is mesh generation. In order to produce accurate results, it is essential to understand the influence of mesh size. Obtaining a completely mesh independent solution could be very expensive and time consuming, particularly if the mesh size is reduced erratically. To have a suitable mesh density for a specific problem with acceptable CPU time and numerical accuracy has remained a major theme in the CFD literature.

Chapter 2

2. Literature Review

A paper done by Erik Bjerklund and Mikael Ohman entitled 'Stability of High Speed Train under Aerodynamic Excitations' thoroughly examines aerodynamic effects on high speed trains and its impact on both comfort of the passenger and stability of the trains. The paper is performed on Swedish high speed trains that are aiming to go at a speed of 250 km/h. The authors tried to closely connects the aerodynamic effects with the vibration dynamics within the train. The authors chose two scenarios to be simulated. The scenario are when two trains meeting each other and a train leaving a tunnel and is hit by a strong wind gust (35 m/s). From the aerodynamic part, computational fluid dynamics (CFD) is used. To simulate both scenarios a moving mesh needs to be used. From the CFD the moments and forces from the pressure and traction on the train body are calculated, and these loads are taking into a low order mathematical model that simulates the vibration dynamics in the train. [8]

In the paper Aerodynamic "Single train passing through a tunnel", Jakub Novák choose to examine aerodynamic impact created by tunnels as the loads represent an integral part of general loads that effect on operating rail vehicles. Highest values of rail vehicle aerodynamic loads can be reached along the entrance and passage through a tunnel. When a train passes through a tunnel, pressure waves are generated which propagate along the tunnel approximately at sonic speed. These pressure variations may pass into the interior of the trains, unless they are pressure sealed, and may cause discomfort to train passengers. The difference of pressure between outside and inside [9]

The train set consists of an electrical loco and three coaches. The loco model shape closely corresponds with a real three-system electrical locomotive developed and produced by ŠKODA. The train performs a straight movement of 200 km/h speed rate. The main goal of the contribution is to monitor both the train motion aerodynamic effects on environment (tunnel wall surface) and backward effects of surrounding objects especially on loco body. Most of the results

represent time variations of pressure, aerodynamic drag and velocities monitored both on tunnel and loco surfaces and in specified locations in the domain. Some of the values computed are compared with admissible limits published in adjacent standards. [10]

The scenario of a train passing through a tunnel has been further investigated in the paper by Florian Guillou. While entering a tunnel the air at the train nose is compressed and it creates an overpressure wave that migrates at the speed of sound. When this waves reaches the end of the tunnel a part of the wave is reflected and goes back as an under pressure wave. As the train tail enters the tunnel an under pressure wave is created and migrates to the end of the tunnel. The pressure variation is maximum when an under pressure wave meets a reflected overpressure wave. The pressure difference reaches then a peak value. [11]

When a train enters a tunnel, a compression wave is induced propagating along the tunnel with sonic speed. This wave is reflected at the opposite portal as a rarefaction wave. When the rear of the train enters the tunnel, a rarefaction wave is produced again propagating along the tunnel relative to the moving air with sonic speed. This wave is reflected at the opposite tunnel end as a compression wave. These two waves are the main waves and they are always reflected at portals with opposite sense. Minor waves are caused by the passage of these waves over the train head and the train tail and so a very complex wave pattern is generated. [11]

Depending on the behavior of the flow, different model can be used. It has to be noticed that the flow can become unstable with a high Reynolds number and the flow becomes chaotic in which the pressure and the velocity change continuously with time within substantial regions. It is the cause of the difference between a laminar and a turbulent flow. If a laminar flow used good and practical model to solve the Navier-Stokes equation, a turbulent flow is difficult to model due to the chaotic behavior of the flow which contains small scales. The flow around a high-speed train becomes turbulent a few centimeters after the front part. [9]

The model used for the different simulations is the k-ω SST model. It is a hybrid solution which uses the k-ε model for the far field and the k-ω model near the wall. The k-ε model takes mainly in consideration how the turbulent kinetic energy is affected. This model has two model

equations, the transport equation for mean turbulent kinetic energy (k) and the transport equation for the dissipation of mean kinetic energy (ε). The dissipation occurs in the smallest eddies. [15]

The flow around the train has been considered as incompressible and was obtained by solving the incompressible form of the unsteady Reynolds-Averaged Navier-Stokes (RANS) equations combined with the realizable k-epsilon turbulence model. In the paper "Aerodynamic characteristics of high speed train under turbulent cross wind: a Numerical investigating using unsteady-RANS method" The flow of turbulent cross wind over a more realistic ICE-2 high speed train model has been simulated numerically by solving the unsteady three dimensional RANS equations. [12]

The simulation has been done in static ground case scenario for different yaw angles. The computed aerodynamic coefficient outcomes using the realizable k-epsilon turbulence model were in good agreement with the experimental data for almost all yaw angles. This study shows that unsteady CFD-RANS methods combined with an appropriate turbulence model can present an important means of assessing the crucial aerodynamic forces and moments of a high speed train under cross wind conditions. The aerodynamic data obtained in this study can be used as a starting point for more advanced studies that investigate influence of strong cross wind on the aerodynamic coefficients of high speed trains while moving either on flat ground or in other dangerous scenarios such as sites with tall viaducts and high embankments. [12]

For the study of single train passing through a tunnel, presented results of numerically solved aerodynamic problem agrees with the presumptions given upon the relevant standards. In a draft of standard4 there is determined a medical health limit, that prescribes the maximum pressure change (peak-to peak) to which train passengers and crew are subjected. It shall not exceed 10 kPa within any part of the time taken by the train to pass through any particular tunnel and operational situation. When looking back, any of the pressure changes presented within this contribution do not reach this value by far. [12]

The maximum (modeled) train speed of motion is not so high to induce such pressure deviations. The tunnel length modeled is not sufficient, increasing length of the tunnel will cause higher

pressure changes. The value of aerodynamic pressure variations considered occur only in extremely rare emergency conditions. Normal rail operations will not involve conditions of this severity. The surface design of the three – system locomotive SKODA is well shaped. As to the problem solved, further effort will be aimed to eliminate "secondary pulsations" (especially of pressure), which occurred when the solution for compressible air flow is the loco head enters into the tunnel realized.

Erik Bjerklund and Mikael Ohman in the stability of high speed train under aerodynamic excitation concluded the scenario with the meeting trains will only cause slight vibrations for the passengers, while the tunnel and side wind has a major impact on the stability of the train. For the side wind at 35 m/s the train would experience too much movement, and at these weather conditions (12 on the Beaufort scale) the train cannot go at full speed due to safety concerns.

In this study the forces from aerodynamic simulations will be used to analyze the behavior of a train with respect stability. Several numerical modeling and simulation will be conducted. A scenario where two trains passes each other, in which case each of the trains contributes further to the existing aerodynamic excitation. This scenario will on the assumption that this two trains passes through an open track. The other scenario is studying the aerodynamic problems occurring when train travels at high speed in tunnel are more complicated and serious compared with the open air traveling. The aerodynamic drag and other aerodynamic loads on the train are strongly dependent on the pressure waves in the tunnel.

The two commercial software tools used for this analysis are CATIAV5 and ANSYS Fluent. CatiaV5 is a general computer aiding drafting, testing and manufacturing system in aerospace and automotive industry. Fluent is a high end computer program modeling fluid flow and heat transfer in complex geometry. Fluent provides complete mesh flexibility, solving flow problems with unstructured meshes that can be generated about complex with relative ease. The train was modeled using catiaV5 software. The dimensions taken from The ERC raw data. The IGES file of the modeled vehicle was taken to ANSYS for mesh generation and transferred to FLUENT for the CFD analysis around the car profile with a vehicle speed of 22.22m/s

Chapter 3

3. Theory of Aerodynamic Simulation

The train aerodynamic problems are closely associated with the flows occurring around train. The flow around the train has been considered as incompressible and was obtained by solving the incompressible form of the steady Reynolds-Averaged Navier-Stokes (RANS) equations combined with the realizable k-epsilon turbulence model. [9] The CFD analysis involves the following fundamental governing equations and the software solves these equations to provide the required results.

3.1. Continuity equation

Consider a specific mass of fluid whose volume V is arbitrarily chosen. If this given fluid mass is followed as it moves, its size and shape may change but its mass will remain unchanged. Hence, one can state that the time-rate-of-change of the integral of the mass of the fluid element is zero as the element moves along with the flow.

$$\frac{\mathrm{D}}{\mathrm{D_t}} \int \rho \mathrm{dV} = 0 \qquad [1]$$

Where, ρ and t are density and time respectively. Applying Reynolds' transport theorem and divergence theorem to the above equation one obtains:

$$\int \mathrm{v} \left\lfloor \frac{\partial \rho}{\partial \mathrm{t}} + \nabla . (\rho \bar{\mathrm{u}}) \right\rfloor \mathrm{dV} = 0 \qquad [2]$$

Where, $\bar{\mathrm{u}}\,(\mathrm{u}, \mathrm{v}, \mathrm{w})$ is the flow velocity vector field. Since the volume is arbitrarily chosen, the only way in which the above equation can satisfied for all possible choices of V is for the integrand to zero then the equation expressing conservation of mass will be given as

$$\left\lfloor \frac{\partial \rho}{\partial \mathrm{t}} + \nabla . (\rho \bar{\mathrm{u}}) \right\rfloor = 0 \qquad [3]$$

The equations which govern the flow over the train are the continuity and Navier-Stokes equations are the mathematical statements of two fundamental physical principles which are conservation of mass and Newton's second law. These governing equations will be derived by applying physical principles to a suitable model of the flow. [12] Depending on the behavior of the flow, different model can be used. It has to be noticed that the flow can become unstable with a high Reynolds number and the flow becomes chaotic in which the pressure and the velocity change continuously with time within substantial regions. It is the cause of the difference between a laminar and a turbulent flow.

If a laminar flow used good and practical model to solve the Navier-Stokes equation, a turbulent flow is difficult to model due to the chaotic behavior of the flow which contains small scales. The flow around a high-speed train becomes turbulent a few centimeters after the front part. The method used in the simulations of this study is the Reynolds-Averaged Navier-Stokes equations model (RANS) which is based on the decomposition of the flow parameters in two components. This decomposition will give the so called Reynolds Averaged Navier-Stokes equation which contains a new term that will be described and interpreted depending on the chosen model. [14]

3.2. The Navier-Stokes Equations

The incompressible Navier-Stokes equations govern the flow around the profile of the rail vehicle. Denote, Sc the car surface, G the ground surface and Ω a large volume around S_c and above G, then using the Einstein notation, the Navier-Stokes equations are written as follows:

- ✓ Incompressibility $\frac{\partial u_i}{\partial x_i} = 0$ on the surface [4]
- ✓ Momentum ($1 \leq j \leq 3$) :

$$\frac{\partial u_j}{\partial t} + \frac{\partial u_i}{\partial x_i}\frac{\partial u_i}{\partial x_i} = \frac{1}{\rho}\frac{\partial P}{\partial x_j} + \frac{\partial}{\partial x_j}\left[v\left(\frac{\partial u_i}{\partial x_j} + \frac{\partial u_j}{\partial x_i}\right)\right] \text{ on surface} \quad [5]$$

Where uj (t,x) , p (t,x) and ρ are respectively the flow velocity, pressure and density. The boundary cinditions for the velocity are of Dirichet type

$$\rho\left(\frac{\partial \mathrm{u}}{\partial \mathrm{t}} + u\frac{\partial \mathrm{u}}{\partial \mathrm{x}} + v\frac{\partial \mathrm{u}}{\partial \mathrm{y}} + w\frac{\partial \mathrm{u}}{\partial \mathrm{z}}\right) = \frac{\partial \sigma_{xx}}{\partial \mathrm{x}} + \frac{\partial \tau_{yx}}{\partial \mathrm{y}} + \frac{\partial \tau_{zx}}{\partial \mathrm{z}} + \rho \mathrm{g}_x \qquad [6]$$

$$\rho\left(\frac{\partial \mathrm{v}}{\partial \mathrm{t}} + u\frac{\partial \mathrm{v}}{\partial \mathrm{x}} + v\frac{\partial \mathrm{v}}{\partial \mathrm{y}} + w\frac{\partial \mathrm{v}}{\partial \mathrm{z}}\right) = \frac{\partial \tau_{xy}}{\partial \mathrm{x}} + \frac{\partial \sigma_{yy}}{\partial \mathrm{y}} + \frac{\partial \tau_{zy}}{\partial \mathrm{z}} + \rho \mathrm{g}_y \qquad [7]$$

$$\rho\left(\frac{\partial \mathrm{w}}{\partial \mathrm{t}} + u\frac{\partial \mathrm{w}}{\partial \mathrm{x}} + v\frac{\partial \mathrm{w}}{\partial \mathrm{y}} + w\frac{\partial \mathrm{w}}{\partial \mathrm{z}}\right) = \frac{\partial \tau_{xz}}{\partial \mathrm{x}} + \frac{\partial \tau_{yz}}{\partial \mathrm{y}} + \frac{\partial \sigma_{zz}}{\partial \mathrm{z}} + \rho \mathrm{g}_z \qquad [8]$$

g_x, g_y and g_z are gravitational accelarion along z, y and z axes. The terms σ and τ are normal and shear stress acting on the fluid, respectively. The first subscript in notaion indicates the direction of the normal to the plane on which the stress acts an the second subscript indicates the direction of the stress.

3.3. Aerodynamic coefficients

When a train cruises in a side wind they experience aerodynamic forces and moments. The aerodynamic forces are the drag force, F_d which resists the forward motion of the train, lift force, F_l which acts upward and tends to raise the train of the rail, and the side force, F_s which pushes the train from the side. The latter is a result of the side wind. The aerodynamic moments that arise due to side wind are the rolling moment M_r the pithing moment, M_p and the yawing moment. Figure 1 show the different aerodynamic forces and moments on a train subjected to a side wind. The magnitude of these forces and moments depends on the Reynolds number and the shape of the train.

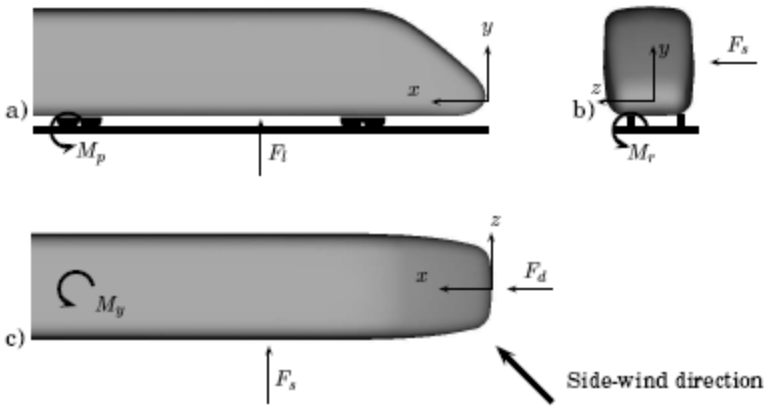

Figure1. Forces and moments acting on trains under the influence [15]

The non-dimensional Aerodynamic side force coefficient (C_s) and the rolling moment friction (Cm) can be calculated as

$$C_s = \frac{F_y}{0.5\rho {V_w}^2 A} \quad [9]$$

$$C_m = \frac{M_x}{0.5\rho {V_w}^2 AL} \quad [10]$$

Where F_y is the force in the y direction, Mx is the moment about the x axis, ρ air density, $V_w$denotes the approaching air speed, A represents the fixed reference area and L represents a fixed reference length.

3.4. Aerodynamic analysis of train/tunnel systems

The aerodynamic problems occurring when train travels in tunnel are more complicated and serious compared with the open air traveling. The aerodynamic drag and noises on the train are strongly dependent on the pressure waves in the tunnel. The aerodynamic drag on a train traveling in a tunnel can significantly increase, compared with that in the open air. A complex wave interaction occurs inside the tunnel due to successive reflections of the pressure waves at the exit and entry to the tunnel. These pressure waves cause large pressure transients resulting in fluctuating loads on the train causing discomfort to passengers.

With the assumption that the cross-sectional areas of train and tunnel are constant, and their equivalent diameters are much larger than tunnel length, and train speed V is very low compared

with the speed of sound corresponding to the atmospheric conditions, and the propagation speed of pressure wave is the same as the speed of sound. Under these assumptions, it is reasonable to prescribe that the continuity equation involves variable density of air but the compressibility effect is not considered in the momentum and energy equations. Assuming that u is the air velocity, and p the pressure, the continuity equation is written as [11]

$$a^2 \frac{\partial u}{\partial x} + \frac{l \partial p}{\rho \partial t} = (\gamma - 1)\varphi \qquad [11]$$

And the momentum equation is given by

$$\frac{\partial u}{\partial t} + \frac{l \partial p}{\rho \partial t} = f \qquad [12]$$

Where 'a' is the speed of sound, the density $'\rho'$ is assumed to be constant, x the distance along tunnel, *t* the time, γ the ratio of specific heats ($\gamma = 1.4$) and f and φ are the frictional force and energy dissipation, respectively, as given in Eqs. [9] and [10]

$$f = \frac{\lambda}{2d} u|u| \qquad [13]$$

$$\varphi = \frac{\lambda}{2d} |u|^3 \qquad [14]$$

For the region in train, the frictional forces stem from both train body and tunnel wall surfaces. Thus, the frictional force and energy dissipation can be expressed as

$$f = \frac{\lambda}{2d} \frac{1}{1-R} u'|u'| - \frac{\lambda'}{2d'} \frac{1}{1-R} (u' - V)|u' - V|, \qquad [15]$$

$$\varphi = \frac{\lambda}{2d} \frac{1}{1-R} |u'|^3 + \frac{\lambda'}{2d'} \frac{R}{1-R} |u' - V|^3 \qquad [16]$$

where d and d' are, respectively, the hydraulic diameters of tunnel and train, and λ and λ' the friction coefficients of tunnel wall and train body surfaces, respectively, R the ratio of the cross-sectional areas of train to tunnel, and u' the flow velocity occurring between train and tunnel.

The compatibility conditions should be used to connect the flow fields in the three regions. Using the coordinate system moving with train, the conservation laws of mass and energy are given by

$$(1-R)(u'-V) = u - V \quad [17]$$

$$p' + \frac{1}{2}\rho(u'-V)^2 = p + \frac{1}{2}\rho(u'-V)^2 = p_o \quad [18]$$

where Cdp is the coefficient of the pressure drag on train in the open air. At the entrance and exit of tunnel, it is assumed that the flow discharges at atmospheric pressure and when the flow comes into tunnel, it is also assumed that the pressure reduces as much as the dynamic pressure.

At the entrance and exit of tunnel, the boundary conditions can be given by

$$(u-V) = (1 - \mathrm{R})(u'-V), \quad [19]$$

$$p + \rho(u-V)^2 = p'(1-R)\rho(u'-V)^2 - C_{dp}R\frac{1}{2}\rho(u'-V)^2 \quad [20]$$

Where, C_{dp} is the coefficient of the pressure drag on train in the open air. At the entrance and exit of tunnel, it is assumed that the flow discharges at atmospheric pressure and when the flow comes into tunnel, it is also assumed that the pressure reduces as much as the dynamic pressure. At the entrance and exit of tunnel, the boundary conditions can be given by

$$tunnel\ entrance\ p = \begin{Bmatrix} \frac{1}{2}\rho u^2, u \geq 0 \\ 0\ ,\ u < 0 \end{Bmatrix} \quad [21]$$

$$tunnel\ exit\ p = \begin{Bmatrix} 0\ ,\ u \geq 0 \\ \frac{1}{2}\rho u^2, u < 0 \end{Bmatrix} \quad [22]$$

The aerodynamic drag on the train travelling in the tunnel is given by

$$\frac{D}{A'} = \frac{1}{2}\rho\begin{Bmatrix} R \\ 0 \end{Bmatrix}(u'-V)^2 + \frac{1}{2}\rho C_{dp}\begin{Bmatrix} (u^2-V)^2 \\ u^2 \end{Bmatrix} + \frac{1}{2}\rho\frac{\lambda'}{d'}\left\{\int_{in}(V-u')|V-u|\,dx + V^2\int_{out}dx\right\} \quad [23]$$

Where D is the aerodynamic drag and A' the cross-sectional area of train. R and 0 in the first term on the right side are, respectively, taken for the fore-body of train to be inside and outside tunnel. Similarly $(u'-V)$ and V^2 in the second term are selected for the after-body of train to be

inside and outside tunnel, respectively. The integral of the third term is performed along train length, and the subscripts in and out indicate the inside and outside tunnel, respectively. In the case where the train is fully outside tunnel, Eq. [19] reduces to Eq. [20] mentioned previously. Before train enters tunnel, the flow velocity and pressure both remain zero. Using these initial conditions, the equations above can be solved after some calculations.

$$\frac{D}{A'} = \frac{1}{2}\rho A' V^2 (C_{dp} + \frac{\lambda'}{d'} l) \qquad [24]$$

A train entering into tunnel at high speed plays a role of the piston motion against the air inside tunnel and thus compresses the air in front of the train. The compression wave will be distorted or weakened by viscous actions and heat transfer inside tunnel [12] When a train of the cross-sectional area ofA' enters a tunnel (cross-sectional area: A) at speed V; a compression wave is formed around the entrance of tunnel. It is assumed that the compression wave form and the resulting pressure rise are expressed as $\Delta P(x)$ and ΔP_{21} $(P_2 - P_1)$; respectively. Where P_1andP_2 are the static pressures just upstream and downstream of the compression wave, respectively. Assuming that the value of ΔP_{21} is very small, compared with the atmospheric pressureP_1; and that isentropic flow is formed between states 2 and 3 [14]

$$\Delta P_{21} = \frac{1}{2}\gamma P_1 {M_t}^2 \frac{1-\emptyset^2}{\emptyset^2+(1-\emptyset^2)M_t-{M_t}^2} \qquad [25]$$

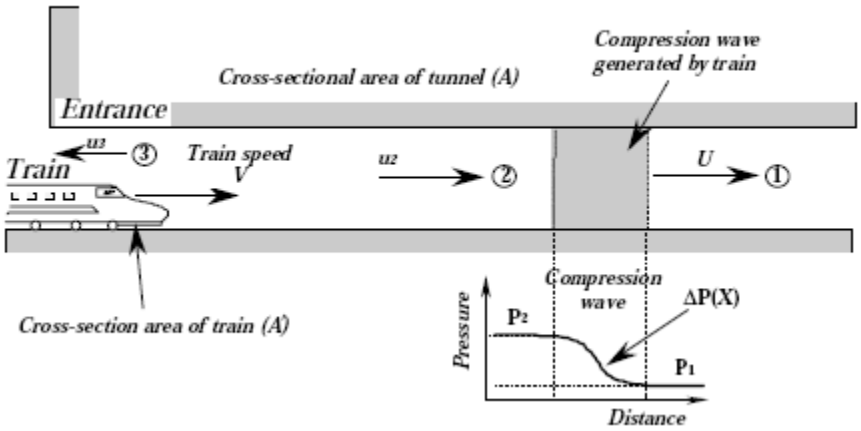

Figure 2. One-dimensional flow model of compression wave [14]

Chapter - 4

4. Modeling and Analysis

4.1. Geometric modeling

The analysis of the aerodynamic properties of a train starts with geometric parameterization of the shape of a train. The car body mainly consists of welded structure supported by stainless steel frame. The train has a total length of 29.5m with a driver control unit at both ends of the train. For the purpose of this study, the 3d model is done using Catiav5 modeling software.

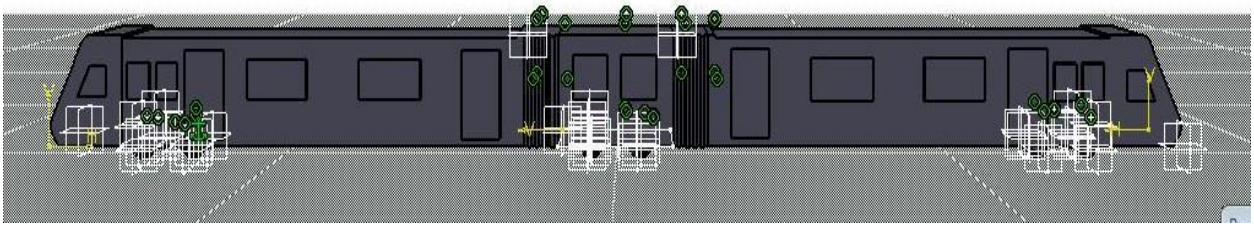

Figure 3 3d model of the train using CatiaV5

4.2. Analysis using ANSYS Fluent

Finite element method produces a greater flexibility to model and analyses complex geometries. It has been widely used in fluid dynamics problems. Air flow gets complex as in flows over a bluff body [Vehicle], the flow becomes turbulent and it is impossible to solve Navier- Stokes and continuity equations analytically. In this thesis the required output is the overall aerodynamics impact and ANSYS Fluent and work the k-e turbulence model with non-equilibrium wall function is selected to analyze the flow over the generic passenger car model. This k-e turbulence model is very robust, having reasonable computational turnaround time, and widely used by the

automotive and railway industry. For the two main scenarios are studied for this research, different computational domain is designated as per the specific requirements.

Steps in Fluent Analysis

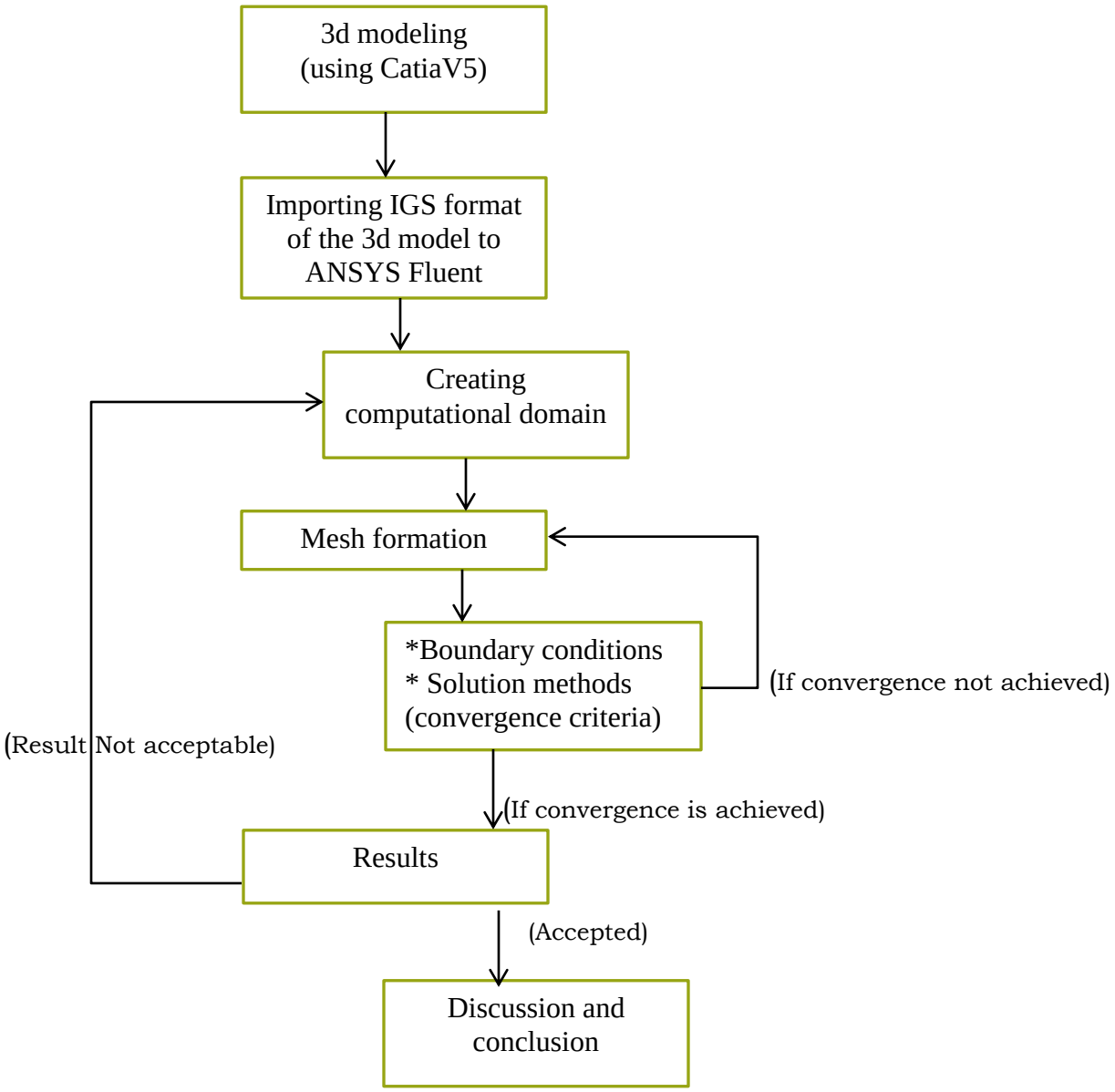

Figure 4. Steps in CFD analysis using fluent

4.2.1. Computational domain for trains passing each other

After the basic shape of the train has been imported to ANSYS, a parallelepiped computational domain is created. Rectangular domain is the most used for automotive and railway industries for the study of aerodynamics as it better simulates the air flow from inlet to outlet. Domain is a requirement for external flows analysis. It is a box filled with fluid and has boundaries. These boundaries are given conditions and the fluid is given a motion. The accurate result from CFD though is impossible but least error can be achieved with an appropriate size of domain. Figure 7 shows a computational domain for two trains which just passed each other.

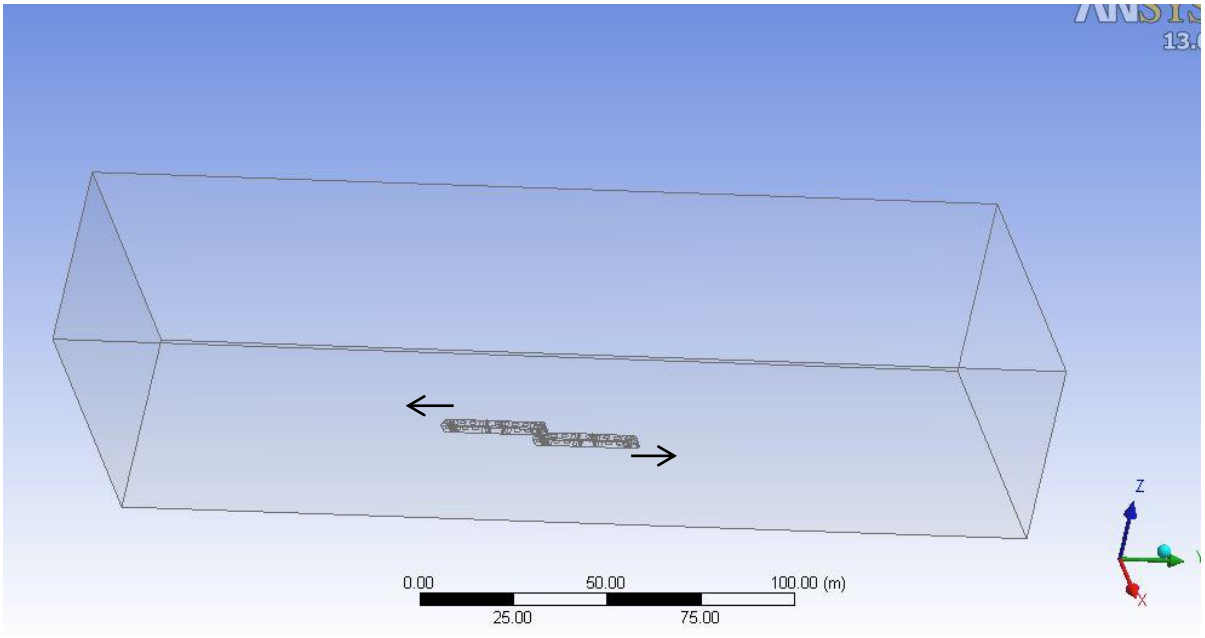

Figure 5 . Computational domain of two trains passing each other

4.2.2. Mesh creation

CFD uses finite volumes method which means that a mesh has to be created. The cells of the mesh contain the information of the flow. A finer mesh leads to a more accurate result but it also means longer computational time and that more computer resources are needed. After the meshing is generated on the surface of the train. Aerodynamic evaluation of air flow over an object can be performed using analytical method or CFD approach.

Table 1. Mesh information

Number of Nodes:	174026
Number of Elements	968810
Edge Length Ratio	Min:1.0574
	Max: 293.599
Minimum Face Angle	Min: 0.104678 [degree]
	Max: 83.8353 [degree

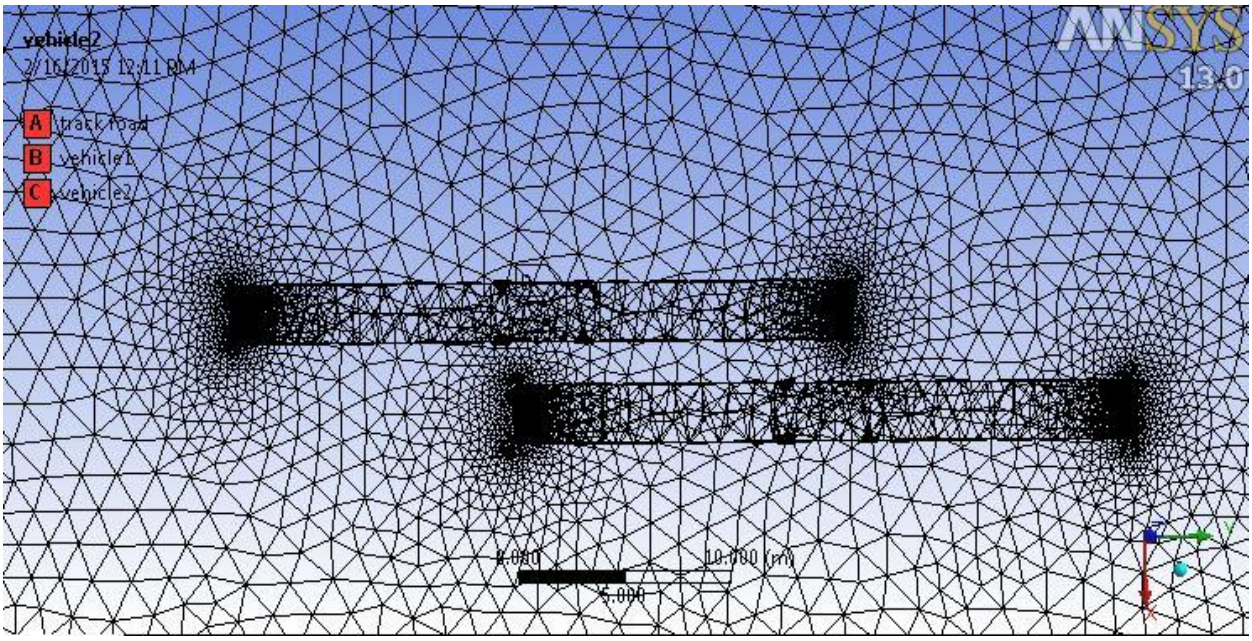

Figure 6. Mesh creation for a scenario train passing each other

For trains passing each other, the paper analyzes three cases in the process of passing eachother. Figure 6 shows a case where the trains are halfway through passing each other. Fig 7 and Fig 8 shows the mesh formation for a scenario entering and exiting a tunnel respectively.

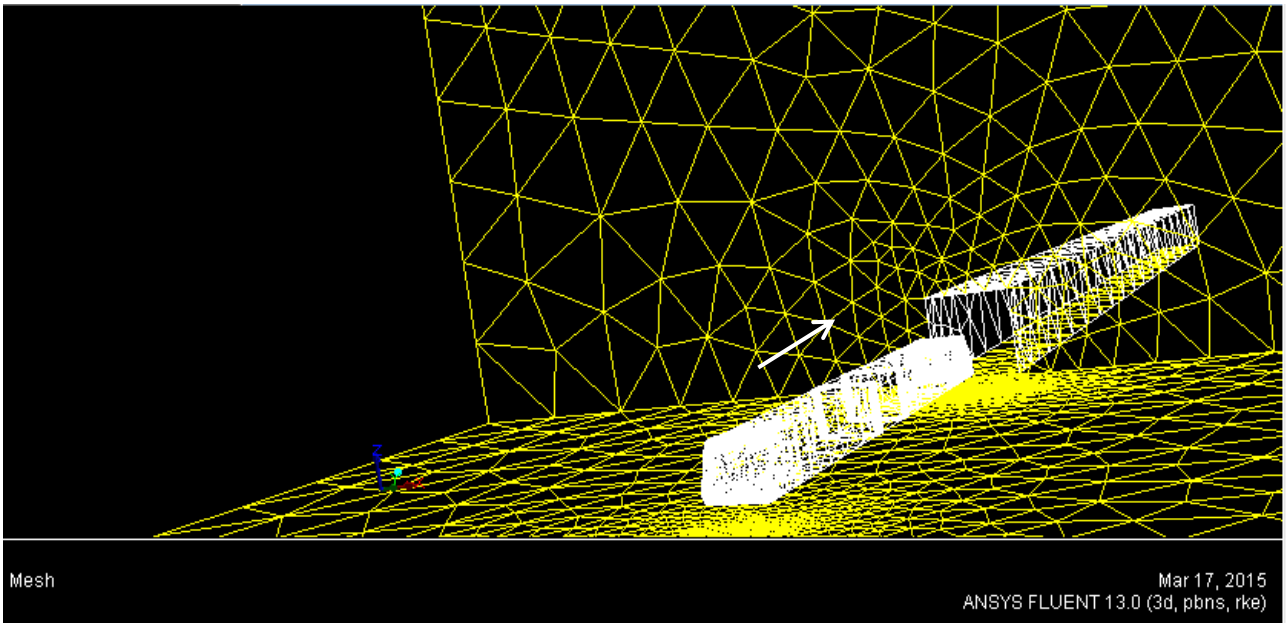

Figure 7. Mesh formation for a train entering the tunnel

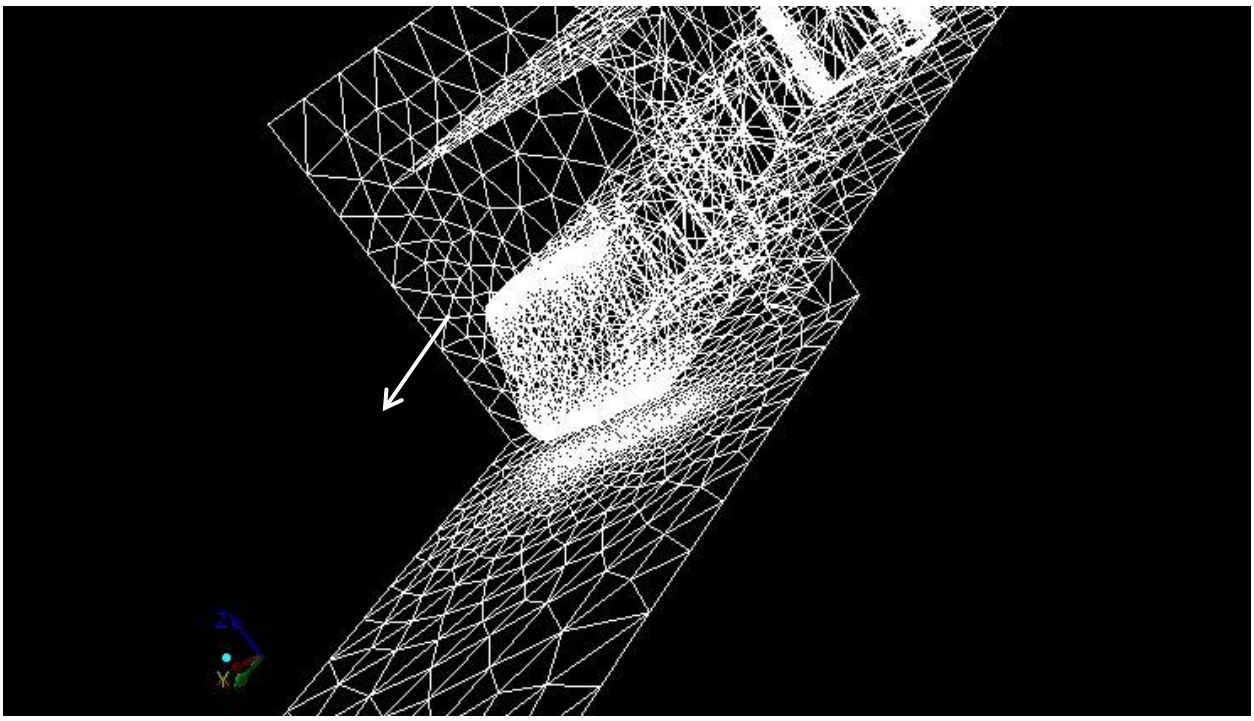

Figure 8. Mesh formation for a train exiting the tunnel

Mesh grids designates the cells or elements on which the flow is solved. It is a discrete representation of the geometry of the problem and has cells grouped into boundary zones where boundary conditions are applied. The grid has a significant impact on:

- Rate of convergence (or even lack of convergence).
- Solution accuracy.
- CPU time required.

Importance of mesh quality for good solutions depends on grid density, adjacent cell length/volume ratios Skewness and boundary layer mesh. For the same cell count, hexahedral meshes will give more, accurate solutions, especially if the grid lines are aligned with the flow. The mesh density should be high enough to capture all relevant flow features. The mesh adjacent to the wall should be fine enough to resolve the boundary layer flow. Three measures of quality Skewness, smoothness (change in size) and aspect ratio. Figure 9 shows the Skewness of the mesh and it shows that the Skewness is least at the nose and tail of the train which makes the mesh formation acceptable as the nose and the tail of the train are the zones where the aerodynamic impact is severe.

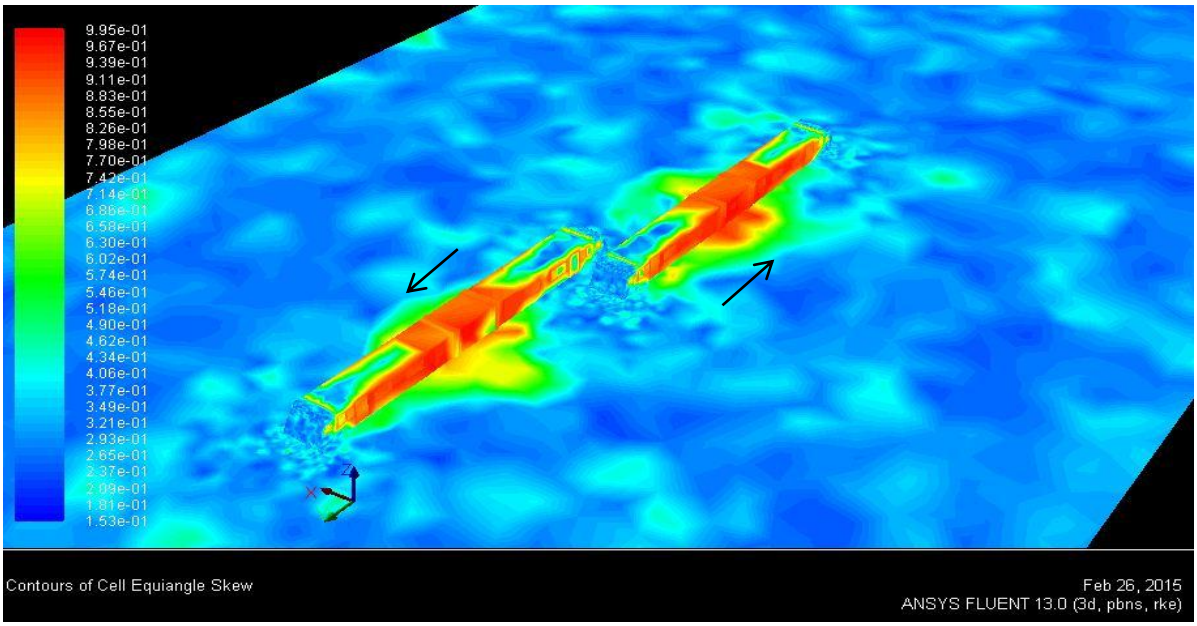

Figure 9. Contour Cell equiangular skew

4.2.3. Solution setup in ANSYS

When we set up for ANSYS simulation, we specify the condition and the direction of the flow. An ANSYS model comprises all the nodes, elements, material properties, real constants, boundary conditions, and other features that are used to represent the physical system. Different boundary conditions are used: wall for all the train, platform and far field, inflow for the inlet and pressure outlet for the outflow.

Table 2. Property of air used in CFD

Property	Units	Method	Value(s)
Density	kg/m3	constant	1.225
Viscosity	kg/m-s	constant	1.79E-05
Molecular Weight	kg/kgmol	constant	28.966

Table 3. Boundary conditions for trains passing each other

Zones name	type
wall-solid	wall
inlet	velocity-inlet
side_symetry1	wall
top_symetry	wall
side_symetry2	wall
outlet	pressure-outlet
vehicle1	wall
vehicle2	wall

Chapter 5

5. Results and Discussion

5.1. Train passing each other

As indicated in the 3d modeling, the length of the train is 29.5m and the figure 10 shows the static pressure distribution along the length of the two trains. The position (-30m) shown in figure 10 is the point where the two trains meet which gives the highest amount of static pressure.

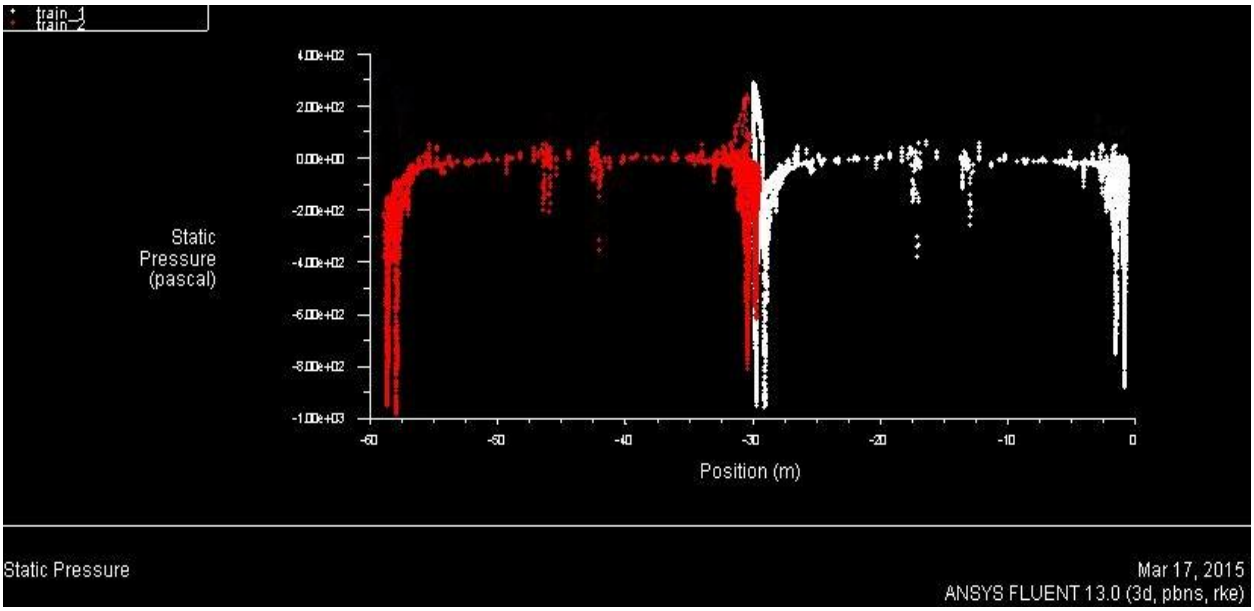

Figure 10. Static pressure graph showing when two trains meet

The static pressure is due to the pressure exerted by the air that is not moving and flowing as a result of a bluff body and it is independent of the velocity of air. In this particular case the air is momentarily trapped at the nose of the train for which the maximum static pressure is exhibited. Figure 11 shows when the two trains meet, the maximum static pressure of 307Pa is exhibited at the front face of the trains and the minimum value of -985Pa is seen at the top edge of the trains.

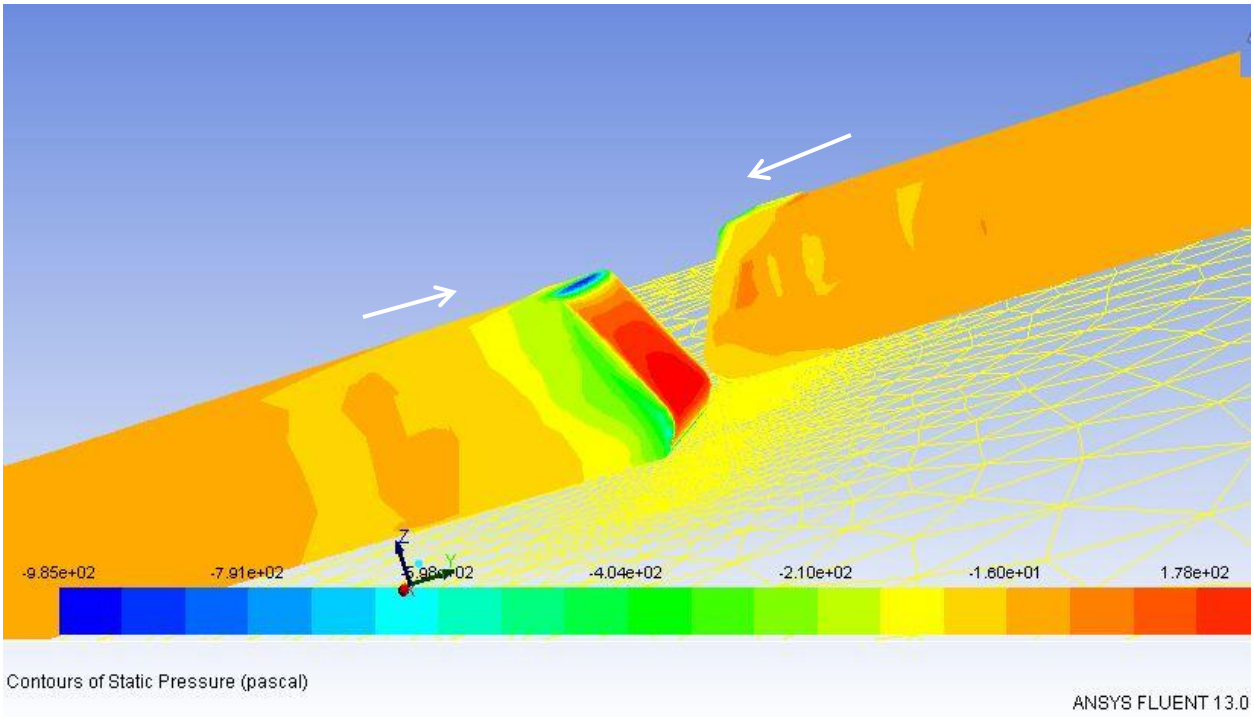

Figure 11. Contour of static pressure when the two trains just met

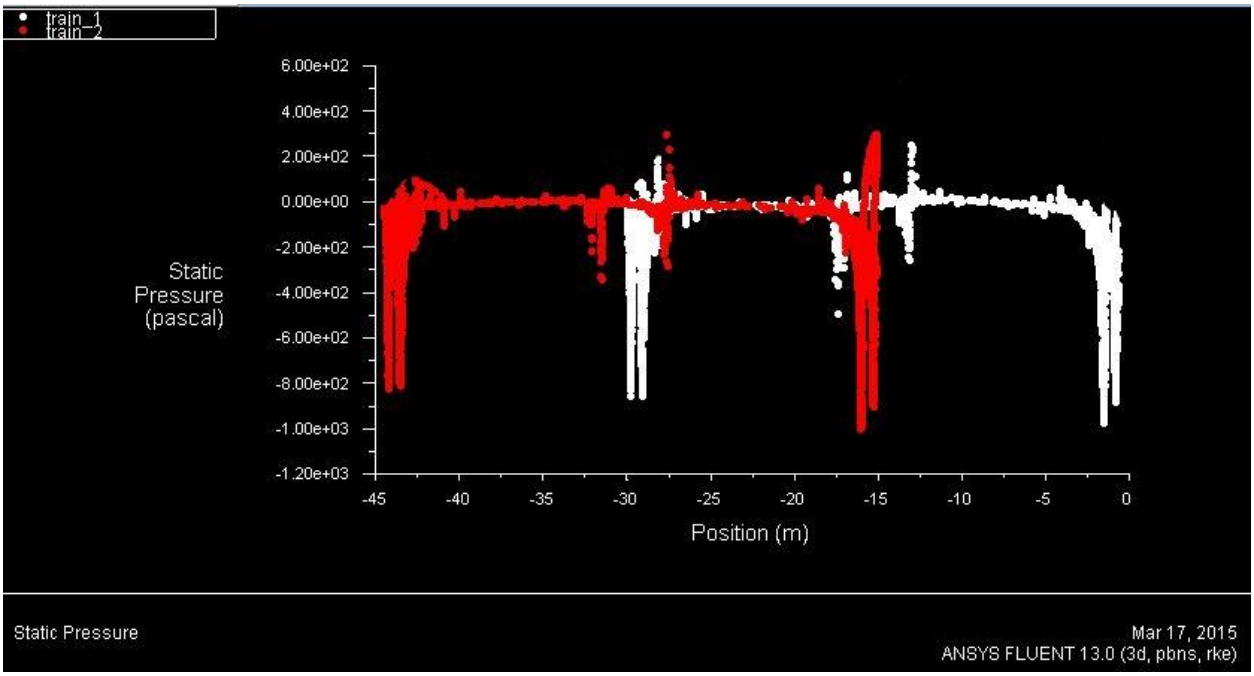

Figure 12. Static pressure graph when the two trains pass halfway through each other

When the trains are half way through, maximum result of static pressure is exhibited at position of -15m and -30m as shown in figure 15. This is due to the nose of train 1 is positioned at -15m and the nose of train two is at -30m.

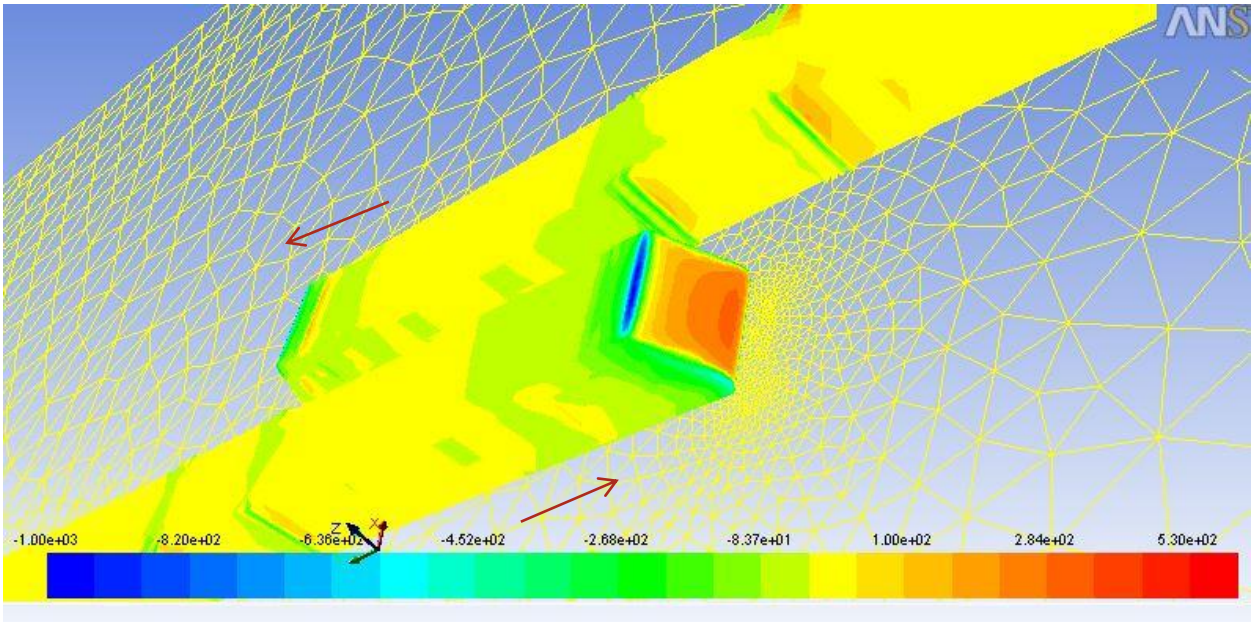

Figure 13. Contour of static pressure when the two trains passed halfway through each other

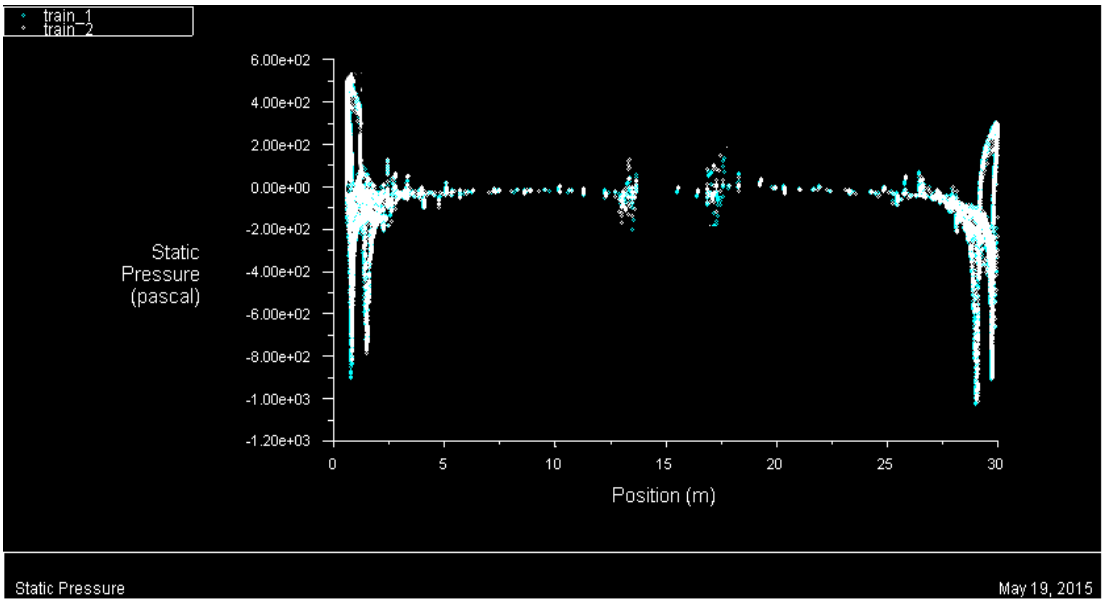

Figure 14. When the two trains are at the same position in the y- axis (along the motion of the train)

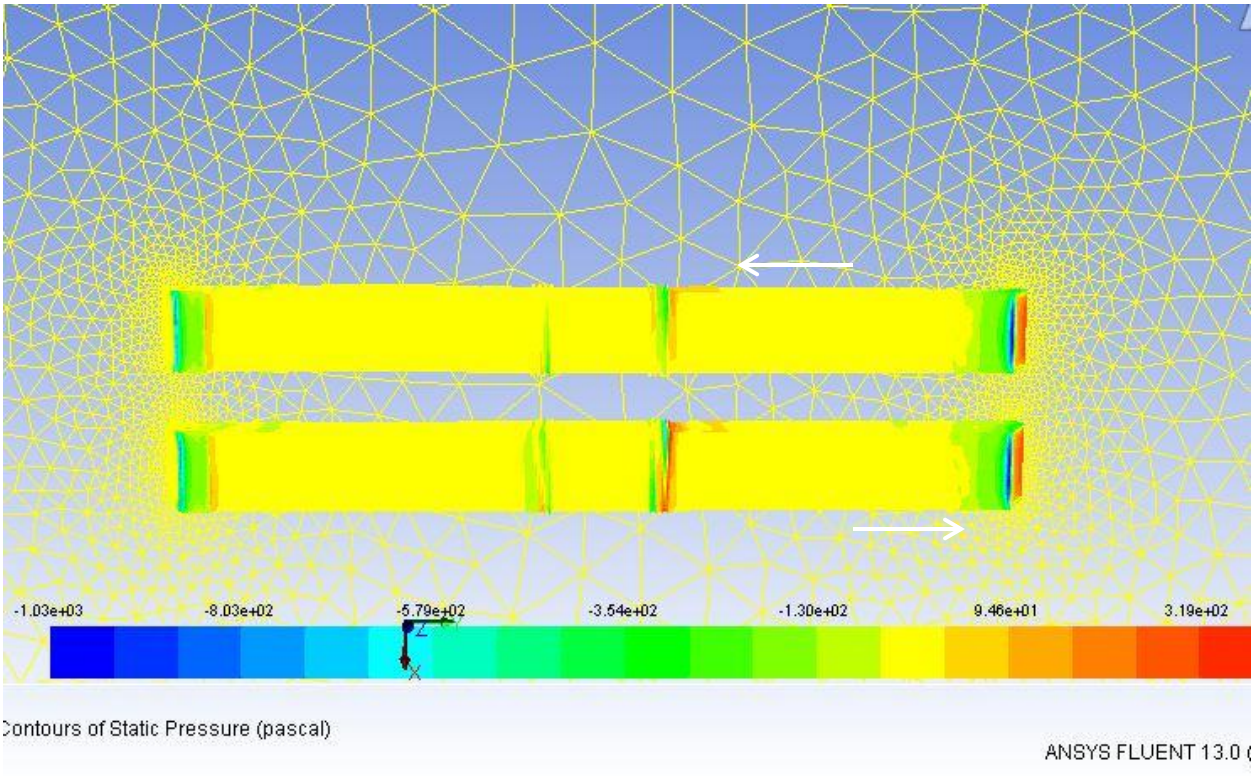

Figure 15. Contour of static pressure when the two trains are at the same position in the y- axis (along the motion of the train)

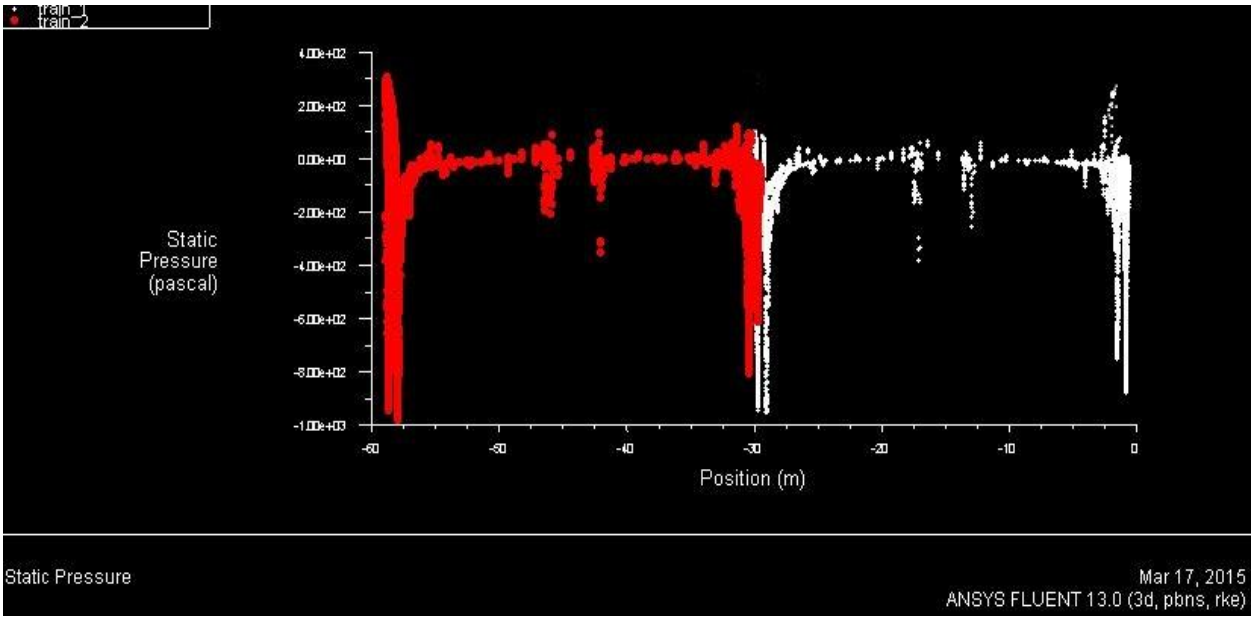

Figure 16. Contour of static pressure when the trains passed each other completely

Figure 19 shows that the nose of the two trains are at 0 and -60m where maximum pressure is exhibited. The tail of the trains is positioned at -30m where the static pressure is significantly high as can be seen on Figure 19 and figure 20.

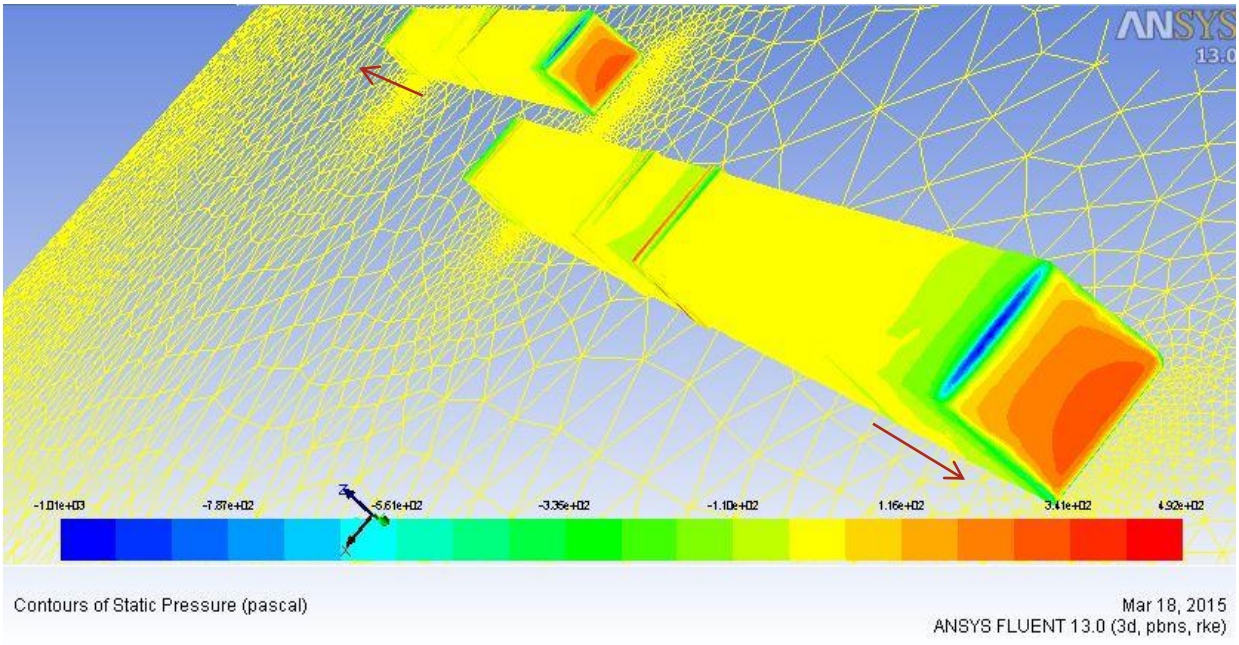

Figure 17. Contour of static pressure when the trains passed each other completely

The surface pressure distributions are computed for all surfaces along the length of the train. As shown in Fig. (14-20) the flow approaches the front edge of the car, it decelerates and then as it negotiates over the top profile of the train, the flow accelerates. This evident from the increasing static pressure towards the front edge and decreasing static pressure on the top rear edge of the train body. When the train is moving, pressure at the top should be significant as this provides stability and to remain the car on ground overcoming the lift.

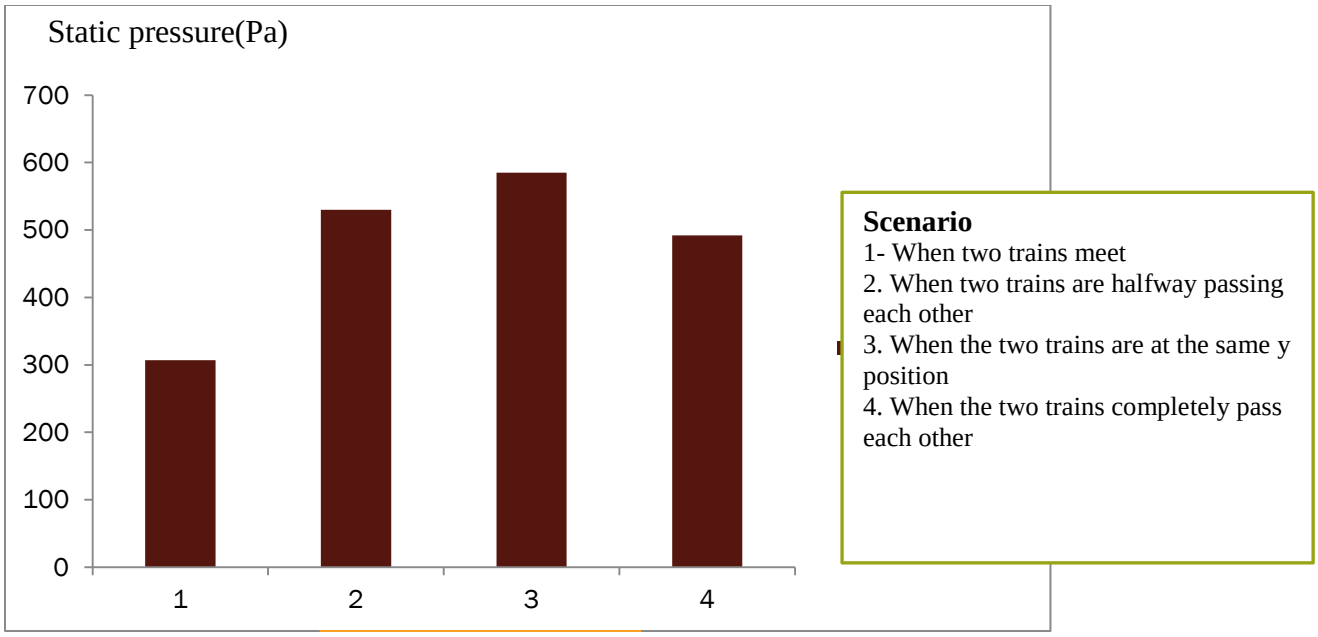

Figure 18. Comparison of static pressure for trains passing each other

Dynamic pressure is the component of fluid pressure that represents fluid kinetic energy (i.e. motion). The dynamic pressure depends on density which is constant for this study and the velocity of the fluid (air)

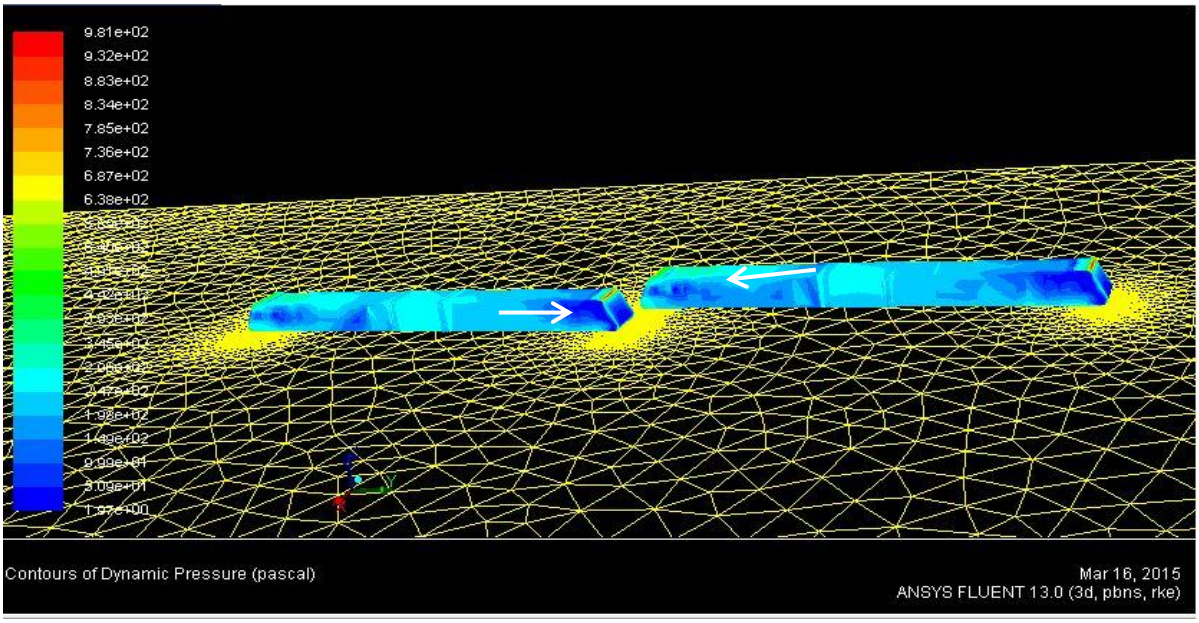

Figure 19. Contour of dynamic pressure when two trains start to pass each other

As indicated in figure 20, dynamic pressure is maximum at the edge of the train, this is due to the air flow is maximum at the edges after being stagnated in the front of the train for few seconds, it will sprint to give the maximum value at the edge and gradually decreases

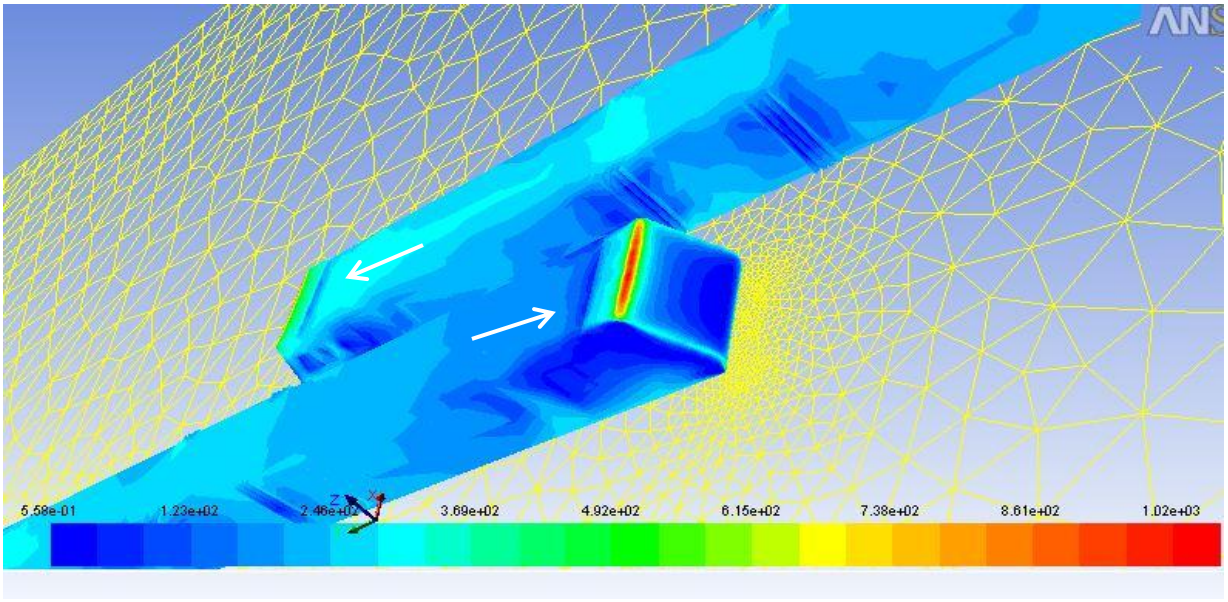

Figure 20. Contour of dynamic pressure when are halfway through when passing each other

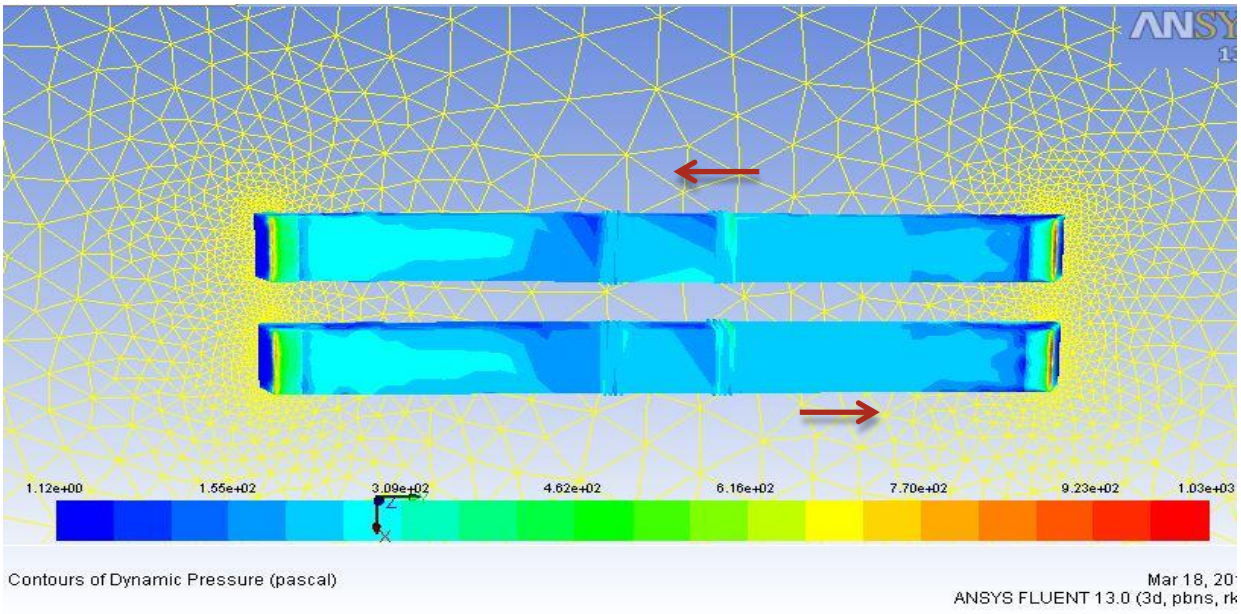

Figure 21. Contour of static pressure when two trains are at the same y position

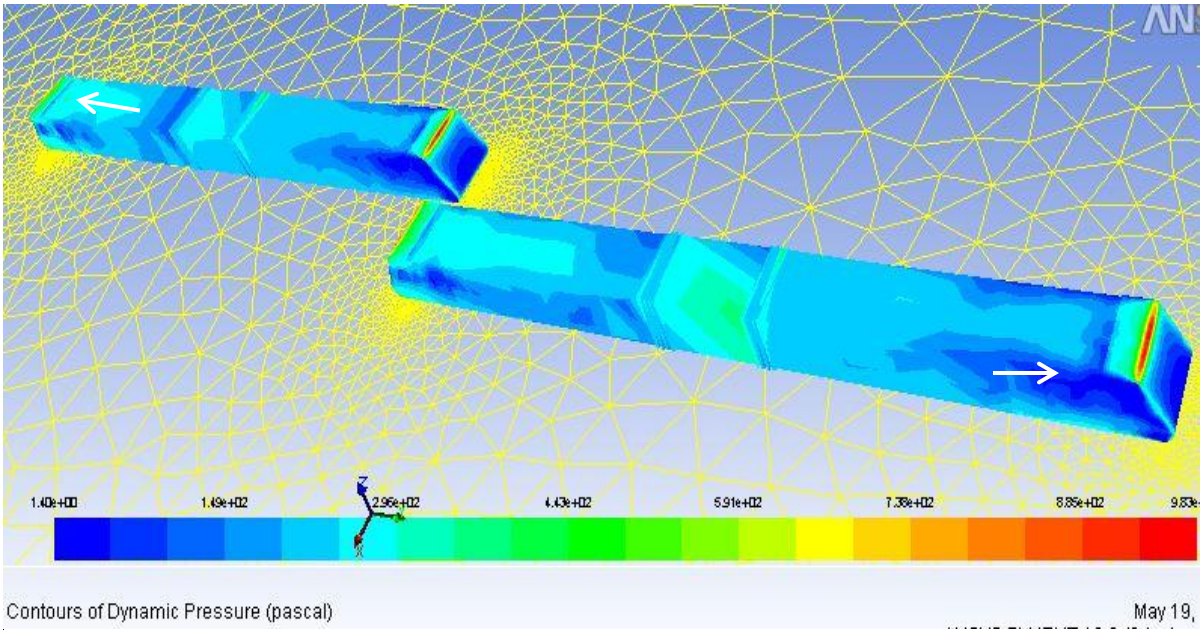

Figure 22. Contour of dynamic pressure when two trains completely passed each other

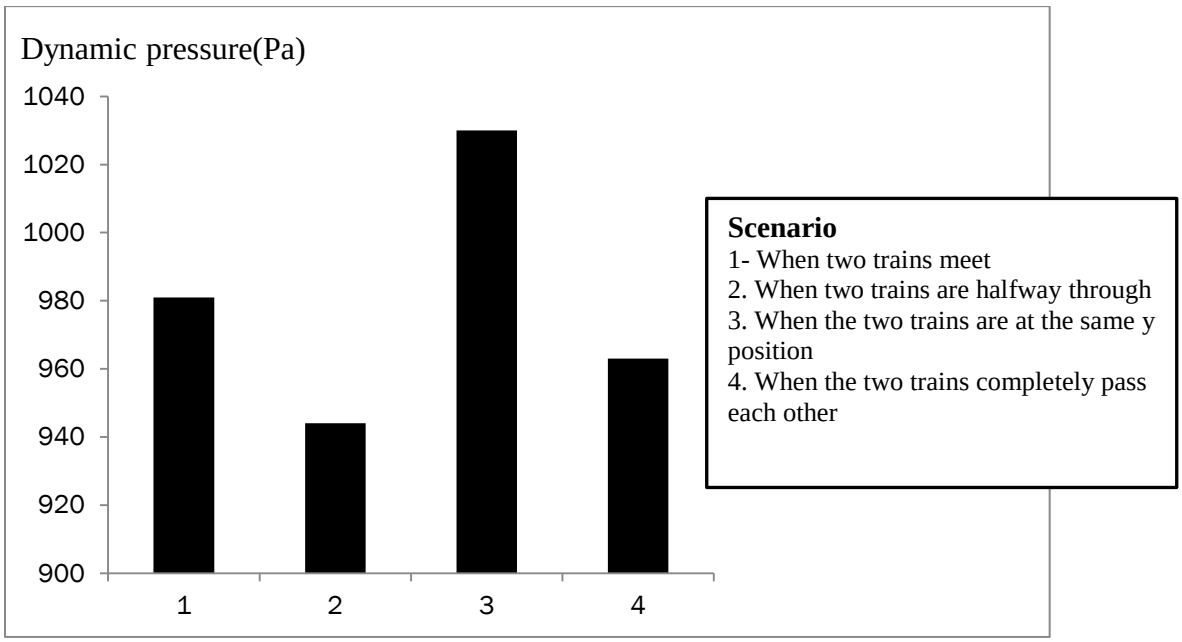

Figure 23. Comparison of dynamic pressure

Taking total pressure into consideration maximum pressure is at the frontal area of the train which gradually reduces towards the rear end of the car. Taking aerodynamic features into consideration coefficient of drag and lift is calculated using the code.

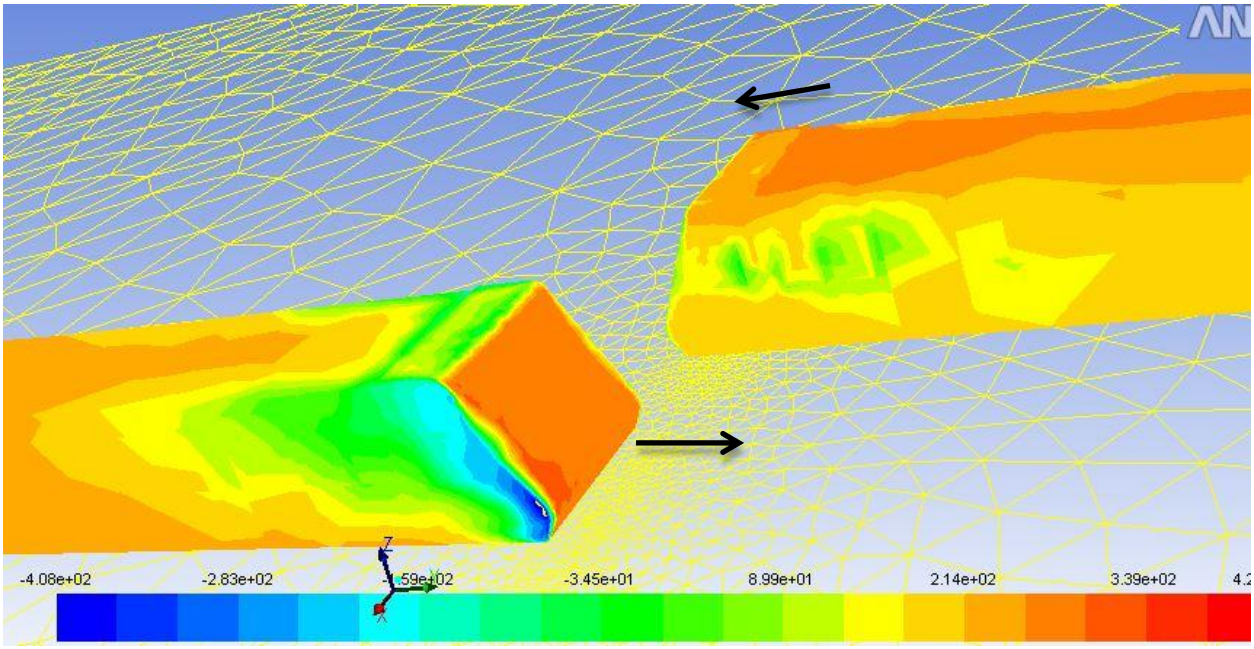

Figure 24. Contour of total pressure when two trains start to pass each other

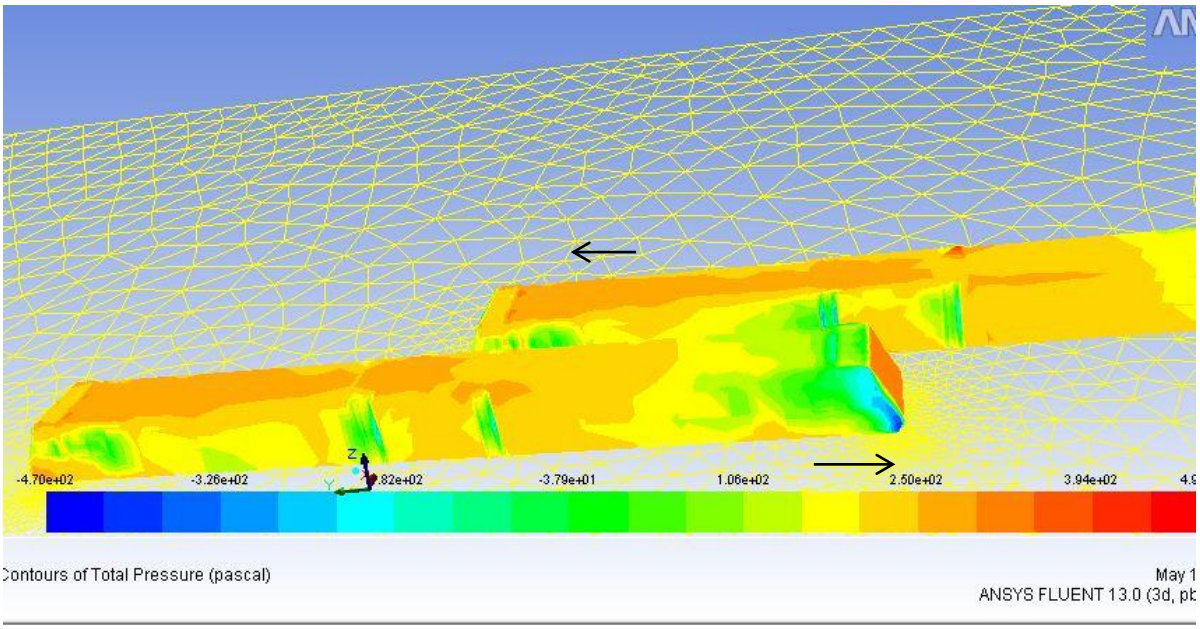

Figure 25. Contour of total pressure when are halfway through when passing each other

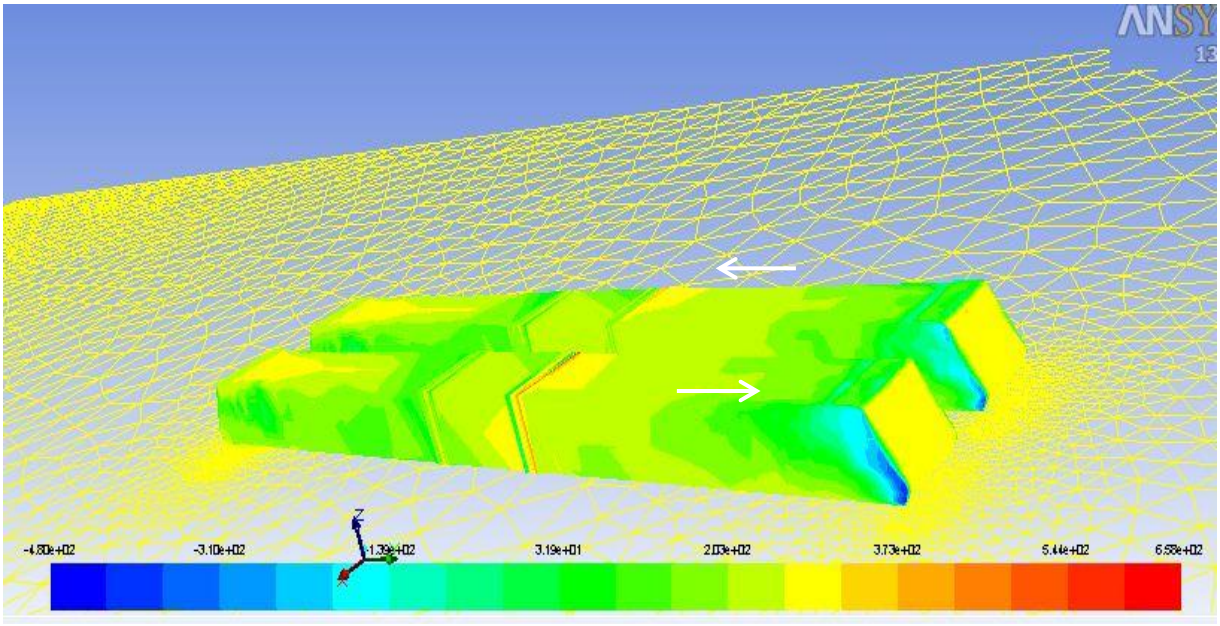

Figure 26. Contour of total pressure when two trains are at the same y position

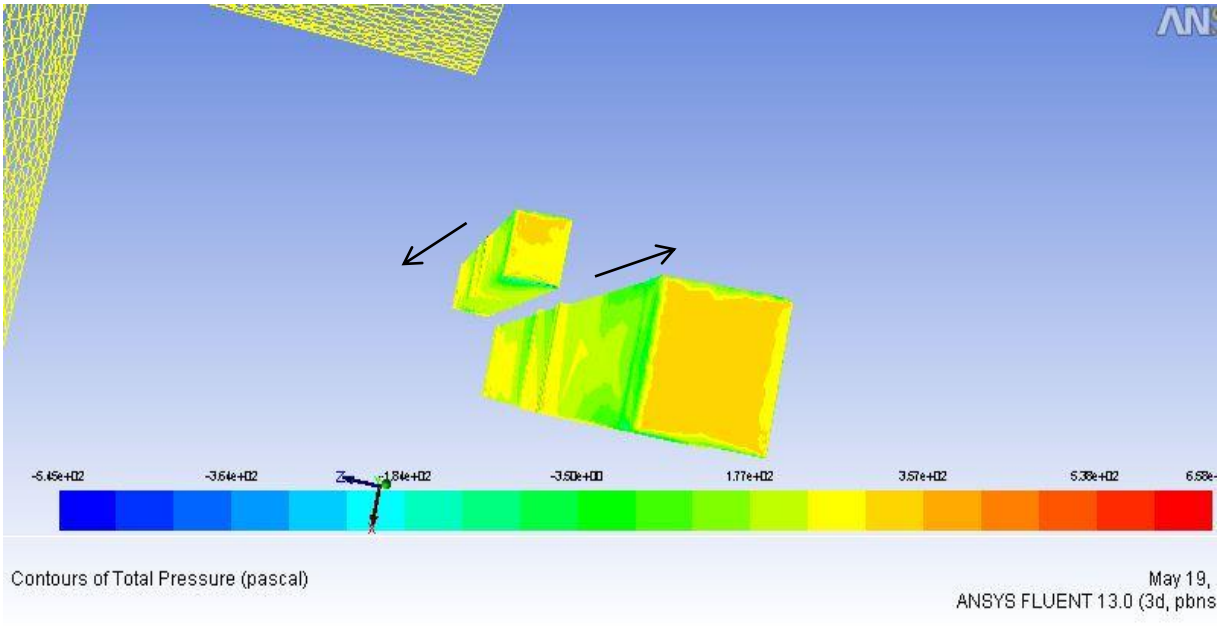

Figure 27. Contour of total pressure when two trains completely passed each other

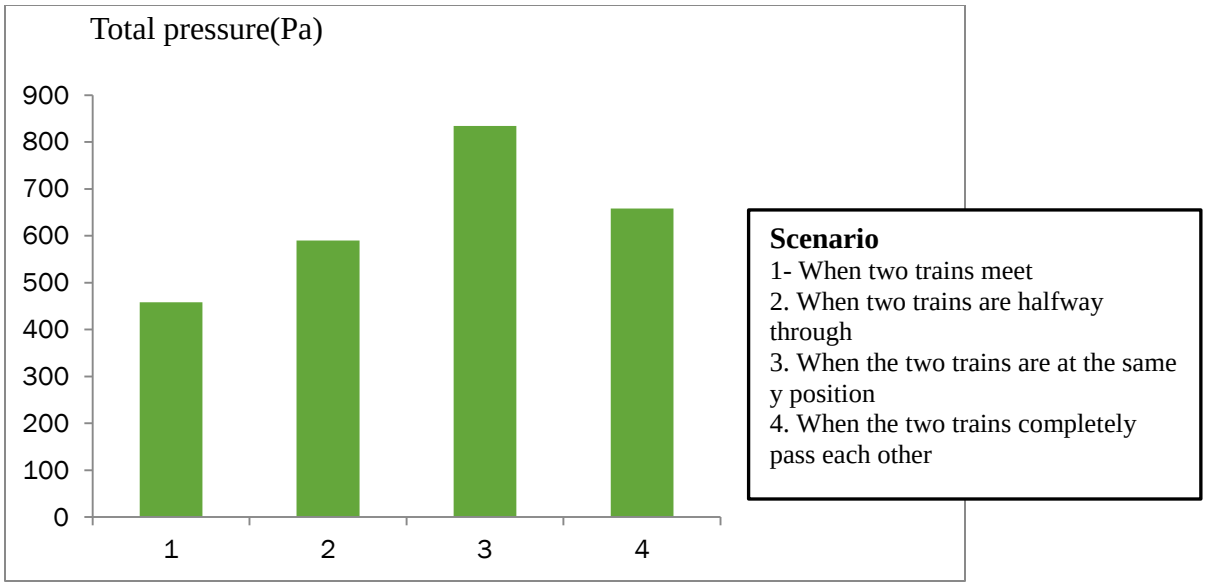

Figure 28. Comparison of total pressure for the 4 scenario

Figure 31shows that velocity is more at the top and is less at the rear and front end of the car. At rear the flow is separating which is the main cause of drag.

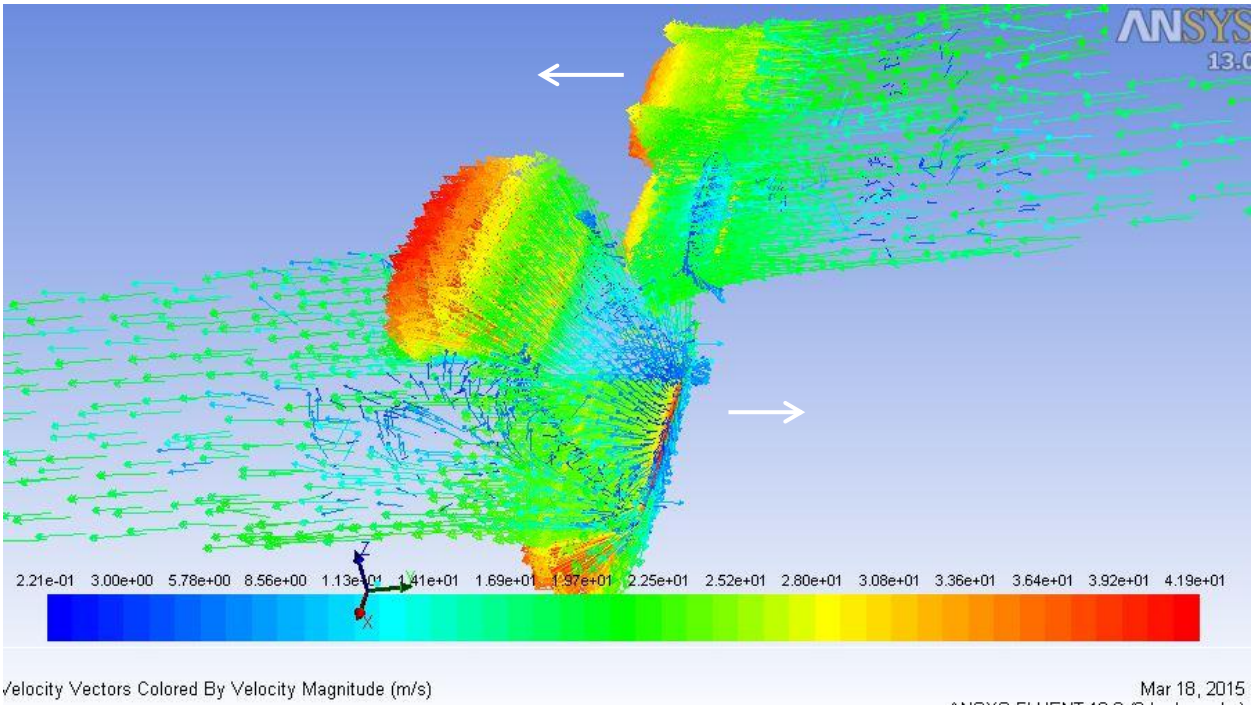

Figure 29. Velocity vector when two trains start to pass each other

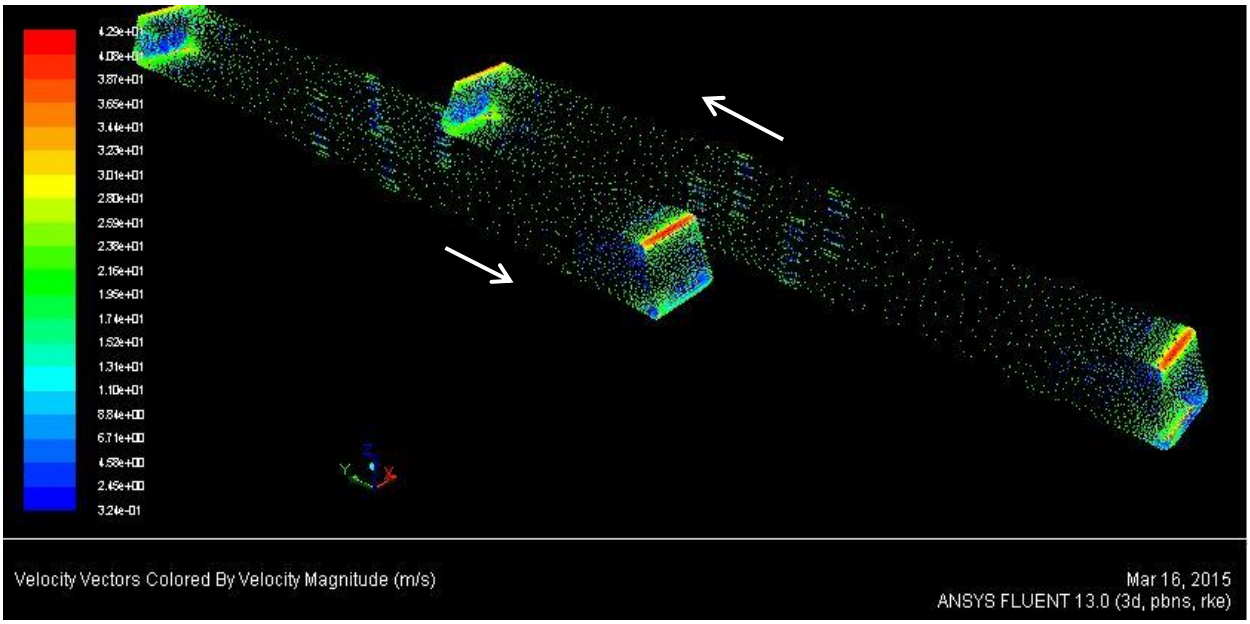

Figure 30. Velocity vector when are halfway through when passing each other

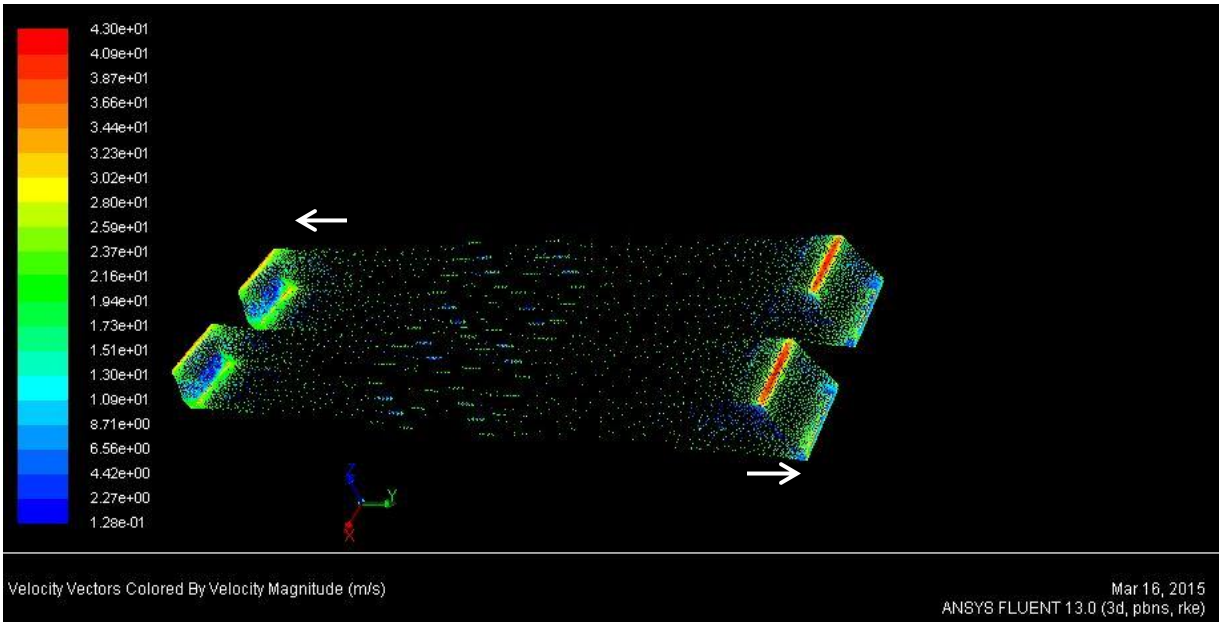

Figure 31. Velocity vector when two trains are at the same y position

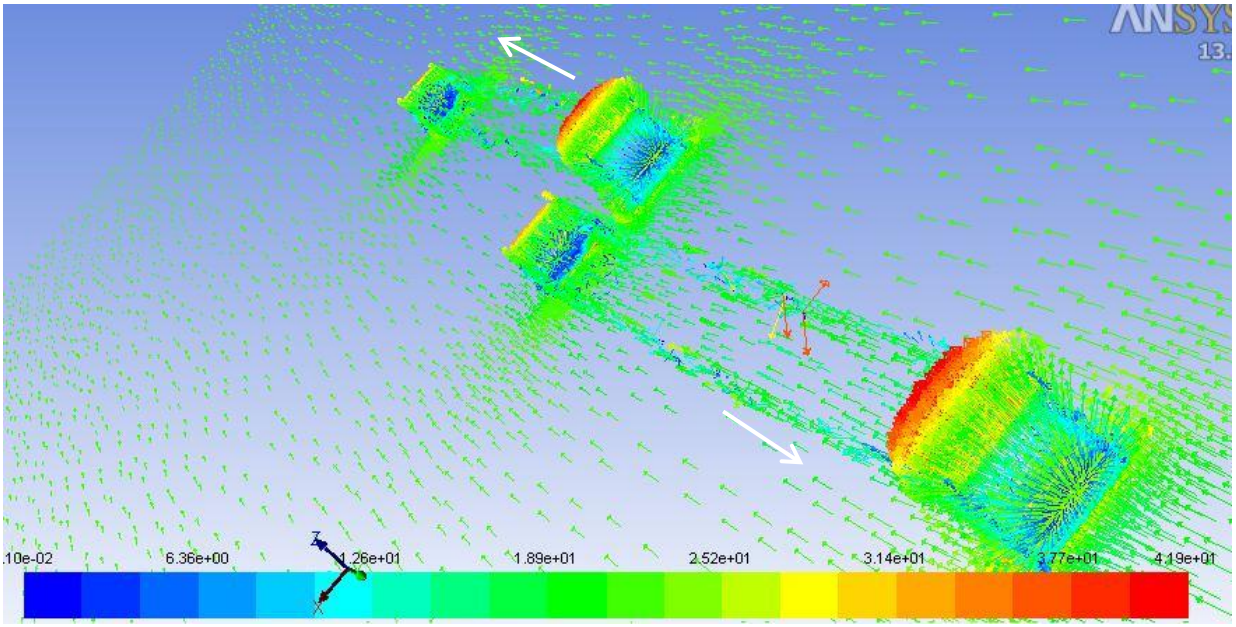

Figure 32. Velocity vector when two trains completely passed each other

5.2. Train passing through the tunnel

5.2.1. Tunnel entrance

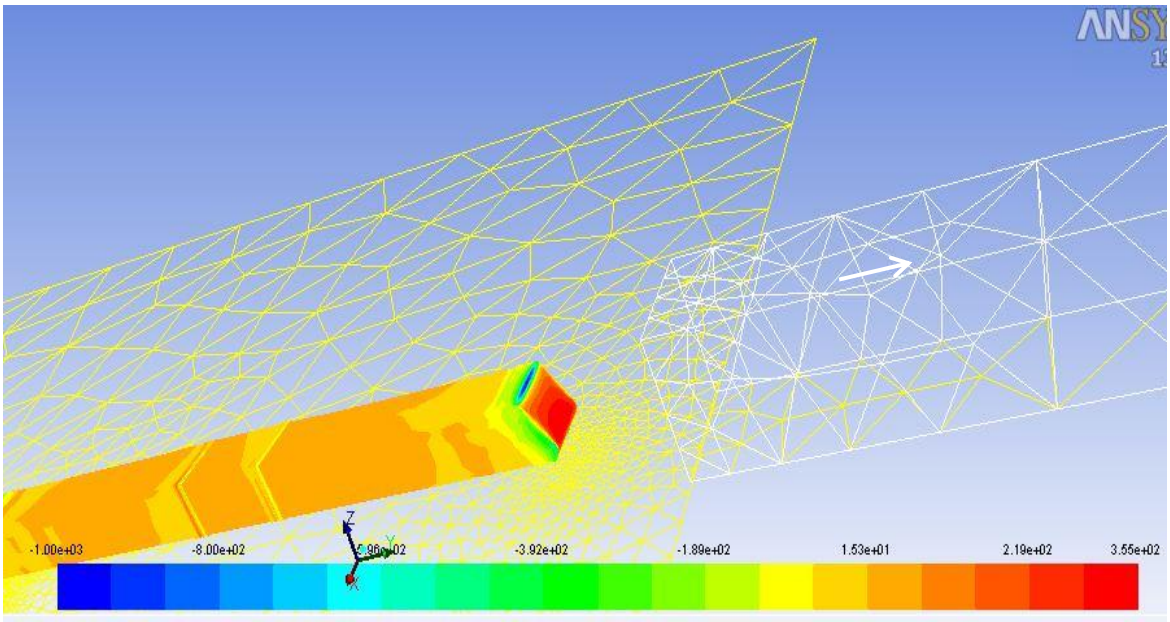

Figure 33. Contour of static pressure for a train entering the tunnel

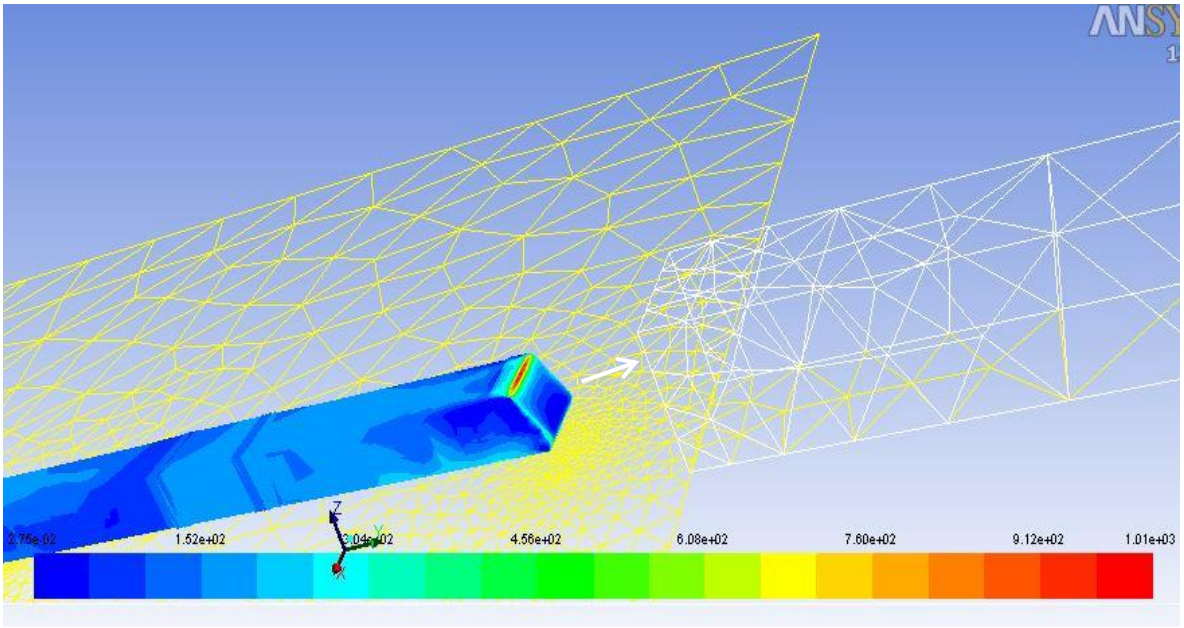

Figure 34 Contour of dynamic pressure for a train entering a tunnel

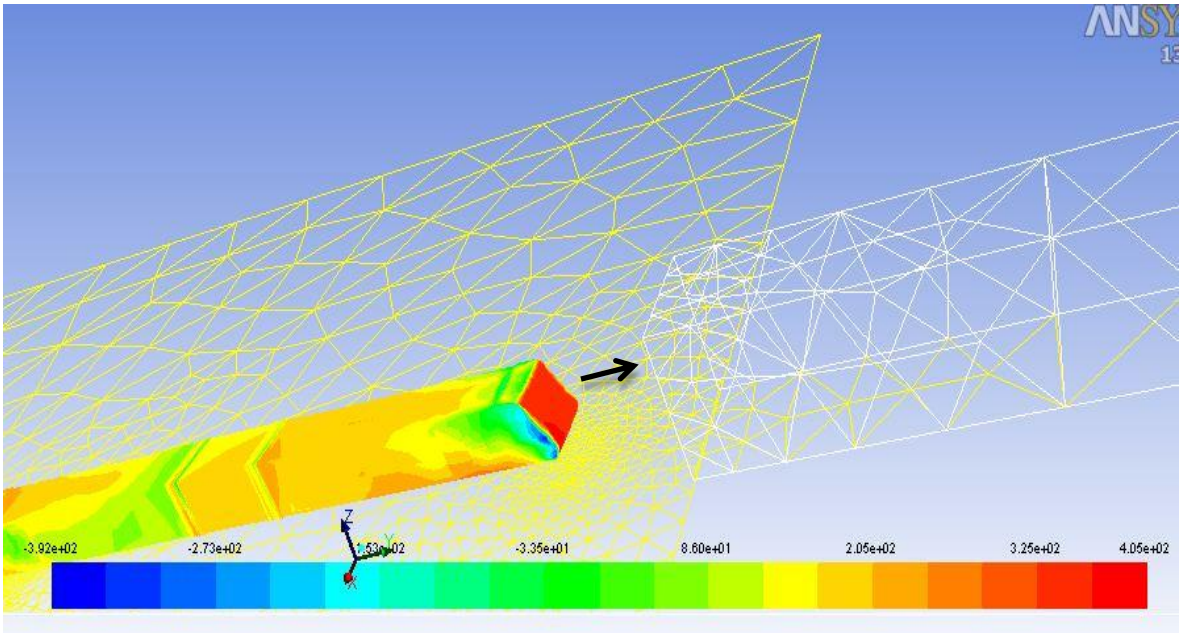

Figure 35. Contour of total pressure for a train entering a tunnel

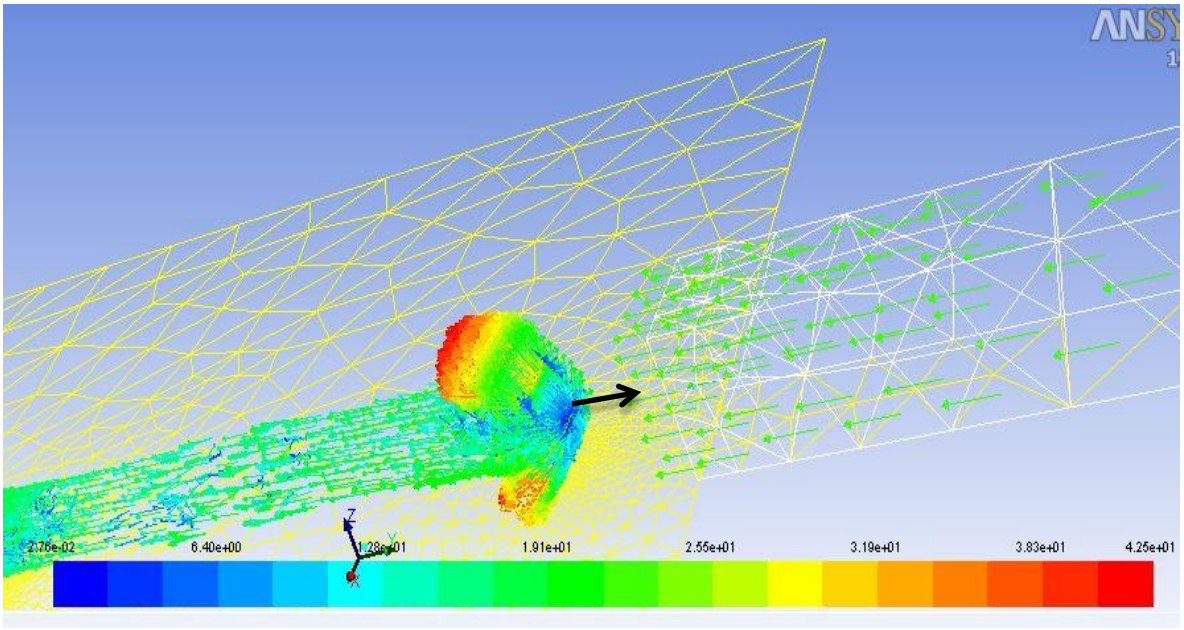

Figure 36. Velocity vector for a train entering a tunnel

5.2.2. Train exiting the tunnel

As the flow analysis results are obtained for a train exiting a tunnel, it is observed that High Pressure points are developed at the front side of the train.

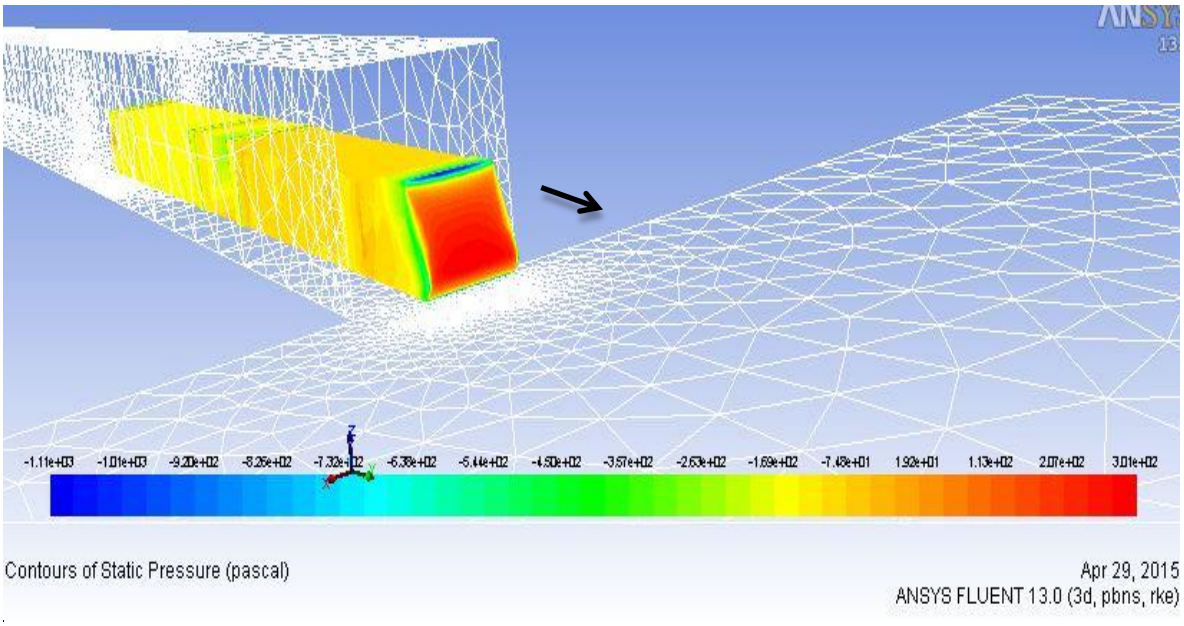

Figure 37. Contour of static pressure for a train exiting a tunnel

When it comes in term of the velocity, it appears that velocity of air films which are in contact with the train don't vary much. But change in velocity is observed above the train. Low velocity zone is obtained right in front of the train air where the air is stagnated. Maximum velocity contour is obtained at the front top of the locomotive. The same behavior is depicted by the velocity vectors. Fair amount of velocity contour is obtained below the train

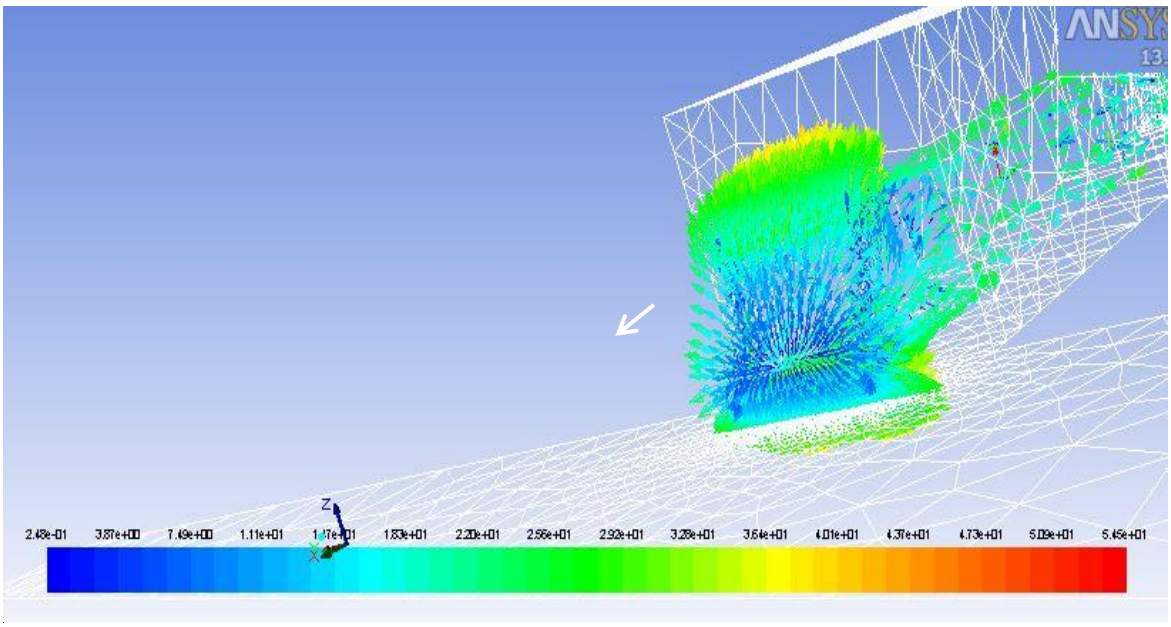

Figure 38. Relative air velocity colored by velocity magnitude

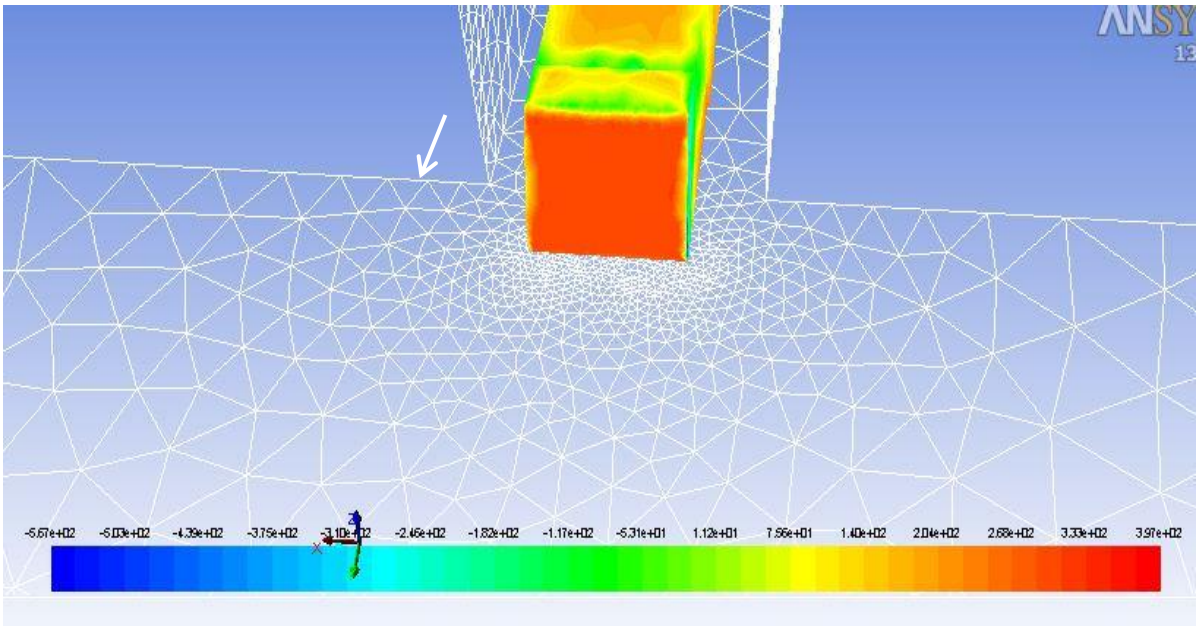

Figure 39 contour of total pressure

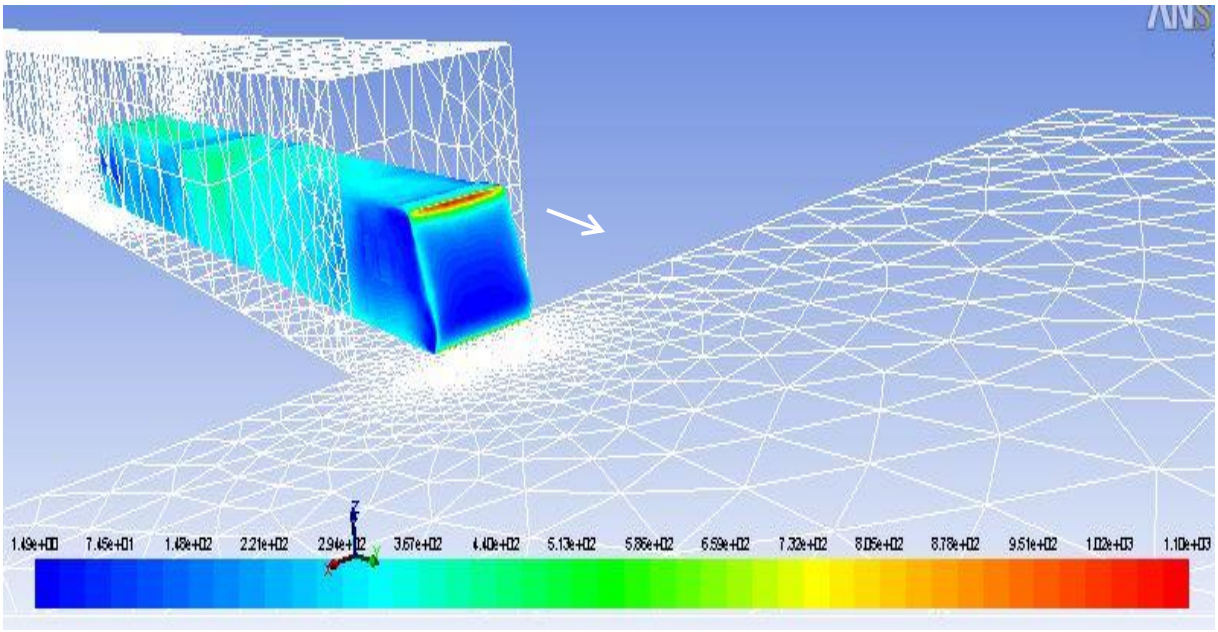

Figure 40 contour of dynamic pressure

5.3. Forces acting on the train

The coefficient of drag and coefficient of lift are shown in figure 44 and figure 45respectively.

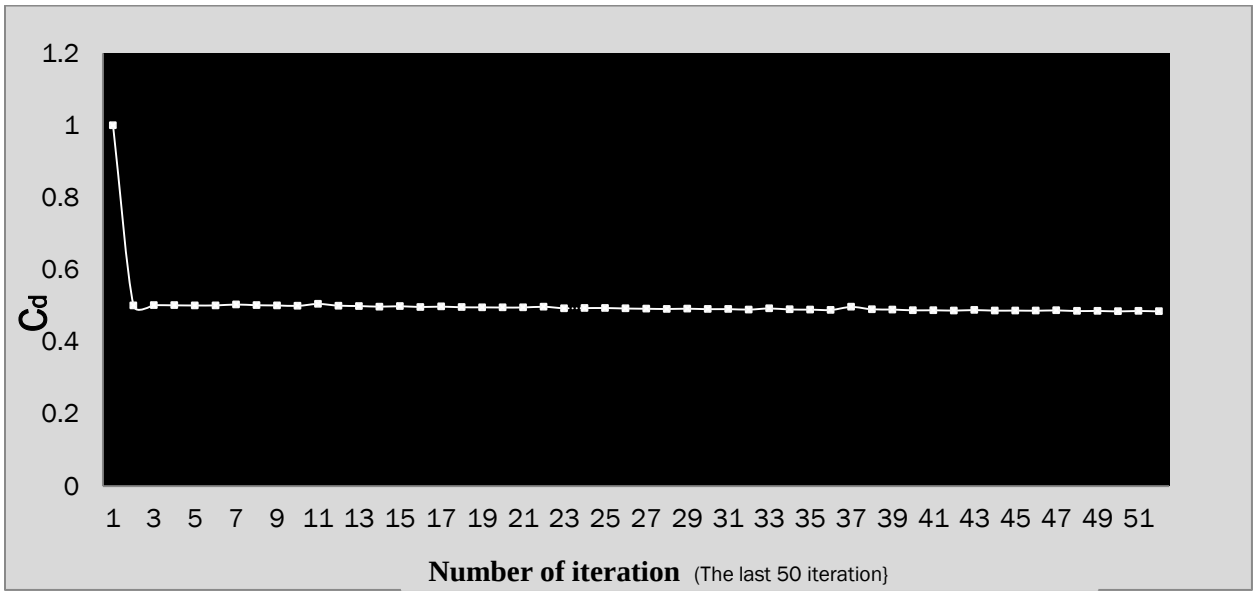

Figure 41. Cd convergence history for the last 50iteration

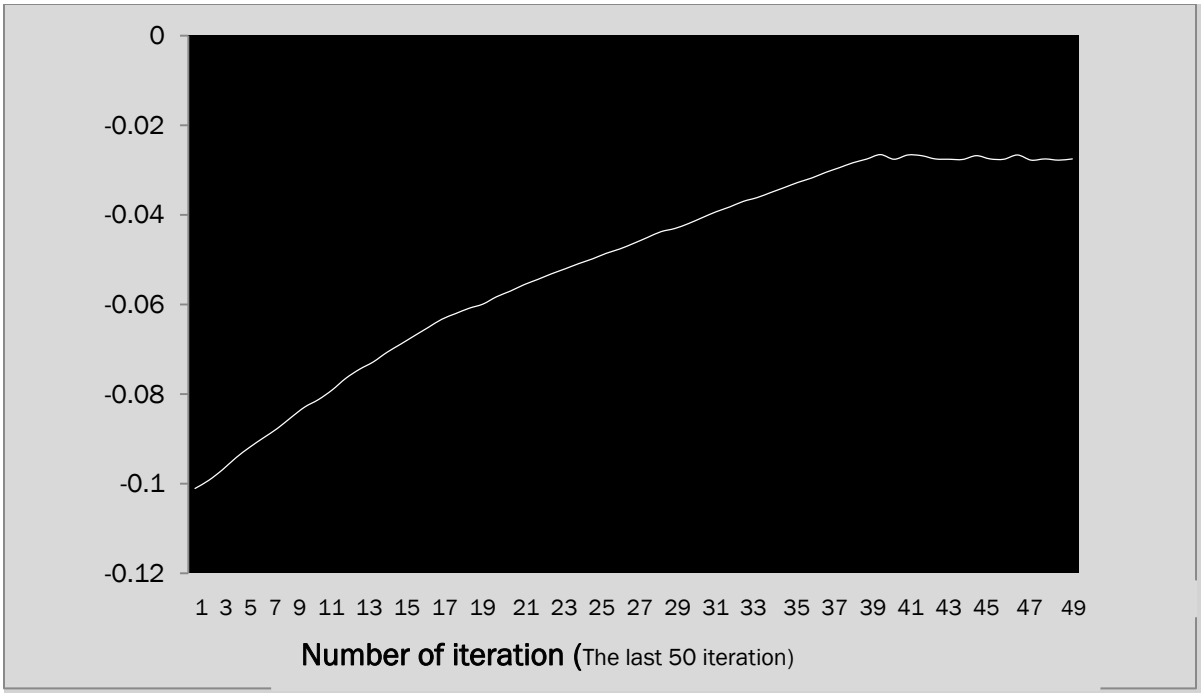

Figure 42. C_l convergence history for the last 50 iteration

When the train runs at high speed, there will be a stagnation region with high pressure on the windward face of the train nose, creating severe drag pressure at the front of the train, we can observe that the drag force acting on the trains on the different scenarios.

Table 4. Drag forces acting on trains when they meet

	Forces(N)		
Zone	Pressure	Viscous	Total
Train 1	1859.28	125.97	1985.25
Train 2	2137.69	121.61	2259.29

Table 5. Lift forces acting on trains when they meet

	Forces(N)		
Zone	Pressure	Viscous	Total
Train 1	-404.90	4.00	-400.90
Train 2	-158.50	5.56	-151.94

Table 6 Drag forces acting on the trains when they are at the same y- position

	Forces (N)		
Zone	Pressure	Viscous	Total
Train 1	2094.45	123.15	2217.60
Train 2	2331.04	123.79	2454.83

Table 7. Forces acting on the trains along z axis when they are at same Y position

	Forces(N)		
Zone	Pressure	Viscous	Total
Train 1	-645.98	2.30	-643.68
Train 2	-508.27	4.07	-504.20

Table 8. Drag forces acting on trains when they already passed each other

	Forces(N)		
Zone	Pressure	Viscous	Total
train_1	2008.67	122.06	2130.73
train_2	2484.07	122.85	2606.92

Table 9. Forces acting on trains along the z- axis when they already passed each other

	Forces(N)		
Zone	Pressure	Viscous	Total
Train 1	-349.34	4.36	-344.97
Train 2	-370.33	3.28	-367.05

Table 10. Drag forces acting on the trains when a train entering the tunnel

	Forces(N)		
Zone	Pressure	Viscous	Total
train	1716.29	97.75	1814.04

Table 11. Lift forces acting on the trains when a train entering the tunnel

	Forces(N)		
Zone	Pressure	Viscous	Total
train	88.38	6.30	94.68

Table 12. Drag forces acting on a train exiting the tunnel

	Forces (N)		
Zone	Pressure	Viscous	Total
train	2737.2239	181.56757	2918.7914

Table 13. Forces acting on the z axis on a train exiting the tunnel

	Forces (N)		
Zone	Pressure	Viscous	Total
train	-427.29889	7.0539351	-420.24495

Chapter – 6

6. Conclusion and Recommendation

6.1. Conclusion

This study is aimed at enhancing our understanding of the stated problem and technical capabilities involved in finding a practical solution for related problems that may arise in NRT or the second phase of A.A.L.R.T projects. When we consider trains passing each other, the scenario where two trains are at the same translational position endure a highest static pressure, this is due to air flow is restricted on the side faces of the train that is nearby each other making the air flow stagnant. In this aforementioned scenario, the peak pressure difference along the train is 1615KPa.

When a train is entering a tunnel, the lift force created is greater than the pressure force that is acting on the top of the train. This is the only scenario where the resultant force in the z axis is positive indicating lift action with a magnitude of 88.7N as indicated in table 11. This amount is however negligent compared to the mass of the train and it has no significant impact on the stability of the train

For a train operating inside a tunnel, the pressure deviation along any part of the train must not exceed 10KPa as subscribed in EN 14067-03. The two scenarios conducted for a train exiting and entering the tunnel shows that the pressure deviation is very low with a magnitude of 1411Kpa and 1355Kp respectively

6.2. Recommendation

In this paper, the aerodynamic impact on trains for different working scenario is studied. It is recommended to add other variables such as vibration while curving and other dynamic conditions to compare the result for stability and comfort. Enhanced capability computers are required to improve mesh for movement. Some information is lost when the mesh is moved far

from the initial position. The mesh quality could also be improved; the automatic mesh generator does not create a perfect mesh and it slightly affects the accuracy of the simulation as a result

6.3. Future works

For further work recommend are the following:

- More velocity tests are needed. The velocities of the meeting trains should be done at several more velocities as well as the velocity of the train and the wind speed for the tunnel scenario.

- Cases with variation of side wind velocity should be performed for different yaw angle. Further effect of wind orientations, varying aspect ratios, varying train geometries as well varying environmental conditions could be analyzed in the future for more responsive solutions.

Reference

1. A. H. Wickens, Taylor & Francis Group, LLC] , 2006, A History of Railway Vehicle Dynamics,
2. Dr. Richard Pankhurst , "The Franco-Ethiopian Railway and its History"
3. Yehualaeshet Jemere (MSc. CEng) Chief Officer, Construction and Project Execution Department July, 2012 Addis Ababa Light Rail Transit Project
4. Gerd Matschke, "Computational Simulation Of Aerodynamic Forces And Side Wind behavior Of Railway Vehicles"
5. Ahmed, H[aseeb] & CHACKO, S[ibi] Computational Optimization of Vehicle Aerodynamics
6. Wolf-Heinrich Hucho , 1993, Aerodynamics Of Road Vehicles Annu. Rev. Fluid Mech. 1993.25 : 485-537 (Ts), Germany
7. Optimization of Aerodynamic Properties of High-Speed Trains with CFD and Response Surface Models by Siniša Krajnović Chalmers University of Technology, Department of Applied Mechanics, Göteborg, Sweden, e-mail: sinisa@chalmers.se
8. Erik Bjerklund Mikael Ohman, 2009, " Stability of High Speed Train under Aerodynamic Excitations" Department of Applied Mechanics Division of Dynamics and Division of Fluid Mechanics CHALMERS UNIVERSITY OF TECHNOLOGY
9. Jakub Novák , 2006 "Single train passing through a tunnel" European Conference on Computational Fluid DynamicsECCOMAS CFD
10. Schulte-Werning, B., Gregoire, R., Malfatti, A. and Matschke, G., 2002, "TRANSAERO: A European Initiative on Transient Aerodynamics for Railway System Optimisation." Springer, ISBN 3540433163, 9783540433163.
11. Florian GUILLOU, "CFD Study of the Flow around a High-Speed Train", Master ThesisKungliga Tekniska Högskolan, Stockholm

12. Asress Mulugeta Biadgo PhD, 2014 "Aerodynamic Characteristics of High Speed Train under Turbulent Cross Winds: a Numerical Investigation using Unsteady-RANS Method" Addis Ababa University Technology Faculty Department of Mechanical Engineering Addis Ababa Ethiopia

13. Wendt, J.F.: Computational Fluid Mechanics: An Introduction, Springer-Verlag, Berlin Heidelberg, 2009.

14. Raghu S. Raghunathana, H.-D. Kimb T. Setoguchic "Aerodynamics of high-speed railway train" a School of Aeronautical Engineering, The Queen's University of Belfast,

15. Hassan Nasr Hemida , 2006 , Large-Eddy Simulation of the Flow around Simplified High-Speed rains under Side Wind Conditions"